TECHNICAL REPORT STANDARD PAGE

1. Report No. **FHWA/LA.09/475**	2. Government Accession No.	3. Recipient's Catalog No.
4. Title and Subtitle Accelerated Loading Evaluation of Foamed Asphalt Treated RAP Layers in Pavement Performance	5. Report Date December 2013	
	6. Performing Organization Code LTRC Project Number: 03-2GT: ALF-4 State Project Number: 736-99-1124	
7. Author(s) Louay N. Mohammad, Zhong Wu, and William M. King, Jr.	8. Performing Organization Report No.	
9. Performing Organization Name and Address Department of Civil and Environmental Engineering Louisiana State University Baton Rouge, LA 70803	10. Work Unit No.	
	11. Contract or Grant No.	
12. Sponsoring Agency Name and Address Louisiana Department of Transportation and Development P.O. Box 94245 Baton Rouge, LA 70804-9245	13. Type of Report and Period Covered **Final Report** **04/03 - 06/08**	
	14. Sponsoring Agency Code	

16. Abstract

Due to a lack of locally produced high-quality stone base materials, the Louisiana Department of Transportation and Development (LADOTD) is continuously seeking alternative base materials in lieu of crushed stones used for roadway construction. This report documents the research efforts conducted at the Louisiana Transportation Research Center (LTRC) regarding foamed-asphalt treated reclaimed asphalt pavement (RAP) alternative base materials and provides detailed information on experiment design as well as conducted field and laboratory tests.

An accelerated pavement testing (APT) experiment was conducted in this study using the Accelerated Loading Facility (ALF) at LTRC's Pavement Research Facility (PRF) testing site. The APT experiment included three different base test sections: the first one contained a foamed-asphalt treated 100 percent RAP base course (FA/100RAP), the second used a foamed-asphalt treated 50 percent RAP and 50 percent recycled soil cement base course (FA/50RAP/50SC), and the third had a crushed limestone base. Despite using different base materials, the three APT sections shared other pavement layers and had a common pavement structure: a 2-in. asphalt wearing course, an 8.5-in. base course, and a 12-in. cement-treated subbase course over an A-4 soil embankment subgrade. Each section was instrumented with one multi-depth deflectometer and two pressure cells for measuring ALF moving load induced pavement responses (i.e., deflections and vertical stresses). To expedite traffic-induced pavement deteriorations, two steel load plates of 2,300-lb. each were added to the ALF load assembly (with a self-weight of 9,750-lb.) specifically at the loading cycle numbers of 175,000 and 225,000, respectively. The instrumentation data was collected at approximately every 8,500 ALF load repetitions; whereas, non-destructive deflection tests (NDT) and surface distress surveys (for surface rutting and cracking) were conducted at every 25,000 ALF load passes. In addition, a series of laboratory engineering performance-based tests was performed to characterize the performance of utilized materials in the APT experiment.

The overall APT results generally indicated that the two foamed-asphalt base materials did not perform better than or as well as the crushed stone base. All three test sections were failed primarily due to the development of surface rutting. I isolated fatigue cracks were observed in localized areas of each test section associated with excessive surface ruts. The crushed stone section reached a rutting failure limit of an average rut depth of 0.5 in. approximately at an ALF loading cycle of 282,000; whereas, the FA/100RAP and FA/50RAP/50SC sections reached the limit at 230,000 and 228,000 repetitions, respectively. However, further analyses based on field measurement results revealed that both foamed-asphalt test sections showed slightly less permanent deformation than the crushed stone section during the first 175,000 ALF load repetitions. The backcalculated in-situ moduli of the two foamed-asphalt base courses were higher than that of the crushed stone base during the loading period when the applied ALF load was at 9,750 lb. Loading was increased after this and unfortunately, as the ALF load levels increased, both foamed-asphalt sections suddenly displayed a significantly higher rate of rutting than the stone section and quickly developed a premature rutting failure.

A Shakedown theory analysis indicated that both foamed-asphalt treated RAP base materials seemed to have a lower shakedown threshold stress than the crushed stone base. It was due to the increase of the ALF load levels after the 175,000 repetitions that caused pavement base stresses higher than the shakedown threshold stresses of the two foamed-asphalt treated RAP base materials and eventually resulted in a stage of incremental collapse (or a sudden rutting failure) for the two foamed-asphalt test sections. In addition, the shakedown analysis also suggested that, as long as keeping the traffic induced stress level below the corresponding threshold stresses (as shown in the case when the ALF load was at a 9,750-lb. level), both foamed-asphalt base materials would have continuously performed better than the stone base.

Due to having excellent performance under a 9,750-lb. ALF load, the foamed-asphalt treated RAP mixtures evaluated in this study may be considered for low volume roads, where the percentage of overloaded heavy truck traffic is relatively low and the environment is relatively dry (or a good drainage system is provided).

17. Key Words Foamed-asphalt treated base, accelerated pavement testing, RAP, moisture susceptibility, shakedown	18. Distribution Statement **Unrestricted. This document is available through the National Technical Information Service, Springfield, VA 21161.**	
19. Security Classif. (of this report)	20. Security Classif. (of this page)	21. No. of Pages 92	22. Price

Project Review Committee

Each research project will have an advisory committee appointed by the LTRC Director. The Project Review Committee is responsible for assisting the LTRC Administrator or Manager in the development of acceptable research problem statements, requests for proposals, review of research proposals, oversight of approved research projects, and implementation of findings.

LTRC appreciates the dedication of the following Project Review Committee Members in guiding this research study to fruition.

LTRC Administrator
William "Bill" King
Materials Research Administrator

Members
Phil Arena
Mike Boudreaux
Jeff Lambert
Masood Rasoulian
Don Weathers
Luanna Cambas
Mark Stinson
Neal West
Said Ismail
Simone Ardoin

Directorate Implementation Sponsor
Richard Savoie, P.E.
DOTD Chief Engineer

Accelerated Loading Evaluation of Foamed Asphalt Treated RAP Layers in Pavement Performance

by

Louay N. Mohammad
Zhong Wu
William M. King, Jr.

Louisiana Transportation Research Center
4101 Gourrier Avenue
Baton Rouge, LA 70808

December 2013

ABSTRACT

Due to a lack of locally produced high-quality stone base materials, the Louisiana Department of Transportation and Development (LADOTD) is continuously seeking alternative base materials in lieu of crushed stones used for roadway construction. This report documents the research efforts conducted at the Louisiana Transportation Research Center (LTRC) regarding foamed-asphalt treated reclaimed asphalt pavement (RAP) alternative base materials and provides detailed information on experiment design as well as conducted field and laboratory tests.

An accelerated pavement testing (APT) experiment was conducted in this study using the Accelerated Loading Facility (ALF) at LTRC's Pavement Research Facility (PRF) testing site. The APT experiment included three different base test sections: the first one contained a foamed-asphalt treated 100 percent RAP base course (FA/100RAP), the second used a foamed-asphalt treated 50 percent RAP and 50 percent recycled soil cement base course (FA/50RAP/50SC), and the third had a crushed limestone base. Despite using different base materials, the three APT sections shared other pavement layers and had a common pavement structure: a 2-in. asphalt wearing course, an 8.5-in. base course, and a 12-in. cement-treated subbase course over an A-4 soil embankment subgrade. Each section was instrumented with one multi-depth deflectometer and two pressure cells for measuring ALF moving load induced pavement responses (i.e., deflections and vertical stresses). To expedite traffic-induced pavement deteriorations, two steel load plates of 2,300-lb. each were added to the ALF load assembly (with a self-weight of 9,750-lb.) specifically at the loading cycle numbers of 175,000 and 225,000, respectively. The instrumentation data was collected at approximately every 8,500 ALF load repetitions; whereas, non-destructive deflection tests (NDT) and surface distress surveys (for surface rutting and cracking) were conducted at every 25,000 ALF load passes. In addition, a series of laboratory engineering performance-based tests was performed to characterize the performance of utilized materials in the APT experiment.

The overall APT results generally indicated that the two foamed-asphalt base materials did not perform better than or as well as the crushed stone base. All three test sections were failed primarily due to the development of surface rutting. I isolated fatigue cracks were observed in localized areas of each test section associated with excessive surface ruts. The crushed stone section reached a rutting failure limit of an average rut depth of 0.5 in. approximately at an ALF loading cycle of 282,000; whereas, the FA/100RAP and FA/50RAP/50SC sections reached the limit at 230,000 and 228,000 repetitions, respectively.

However, further analyses based on field measurement results revealed that both foamed-asphalt test sections showed slightly less permanent deformation than the crushed stone section during the first 175,000 ALF load repetitions. The backcalculated in-situ moduli of the two foamed-asphalt base courses were higher than that of the crushed stone base during the loading period when the applied ALF load was at 9,750 lb. Loading was increased after this and unfortunately, as the ALF load levels increased, both foamed-asphalt sections suddenly displayed a significantly higher rate of rutting than the stone section and quickly developed a premature rutting failure.

A Shakedown theory analysis indicated that both foamed-asphalt treated RAP base materials seemed to have a lower shakedown threshold stress than the crushed stone base. It was due to the increase of the ALF load levels after the 175,000 repetitions that caused pavement base stresses higher than the shakedown threshold stresses of the two foamed-asphalt treated RAP base materials and eventually resulted in a stage of incremental collapse (or a sudden rutting failure) for the two foamed-asphalt test sections. In addition, the shakedown analysis also suggested that, as long as keeping the traffic induced stress level below the corresponding threshold stresses (as shown in the case when the ALF load was at a 9,750-lb. level), both foamed-asphalt base materials would have continuously performed better than the stone base.

Due to having excellent performance under a 9,750-lb. ALF load, the foamed-asphalt treated RAP mixtures evaluated in this study may be considered for low volume roads, where the percentage of overloaded heavy truck traffic is relatively low and the environment is relatively dry (or a good drainage system is provided).

ACKNOWLEDGMENTS

IMPLEMENTATION STATEMENT

In a field environment, this experiment demonstrated that foamed-asphalt treated RAP base materials are highly associated with moisture susceptibility problems. Such materials are not recommended for any pavements with a constantly wet subgrade or poor drainage system. On the other hand, the foamed-asphalt treated RAP base materials could perform better than a stone base under a regular 18,000-lb. truck load. Cautions should be taken when using a foamed-asphalt treated RAP base material in Louisiana. The foamed-asphalt treated RAP mixtures should only be considered for low volume roads, where the percentage of overloaded heavy truck traffic is relatively low and the environment is relatively dry (or a good drainage system is provided). In addition, more research on foamed-asphalt mix design to improve water susceptibility of foamed-asphalt treated RAP and other recycled materials is recommended.

TABLE OF CONTENTS

LIST OF TABLES

LIST OF FIGURES

INTRODUCTION

The current LADOTD specification calls for a Class-II crushed stone base layer in its flexible pavement construction. Due to the lack of high-quality stone aggregates and steadily rising costs of imported stone materials, LADOTD is continuously seeking alternative base materials in lieu of a regular stone base. This report documents the laboratory and field performance of foamed-asphalt treated RAP base materials. It is noted that this report is one of a series of reports that documents the results of a recently completed APT experiment conducted at the LTRC's Pavement Research Facility (LTRC Research Project No. 03-2GT: Accelerated Loading Evaluation of a Sub-base Layer on Pavement Performance).

Literature Review

The foamed-asphalt treatment is a process that combines hot asphalt and a small quantity of water in a chamber to produce asphalt foams that are incorporated into a base material. Foamed-asphalt has been used sporadically in the United States since the late 1960s. The foamed-asphalt for use in pavement stabilization was invented in 1957 by Professor Csanyi of Iowa State University [1]. Csanyi's original work demonstrated the effectiveness of preparing low-cost mixes by stabilizing marginal local aggregates such as gravel, sand, and loess with controlled asphalt foam produced by introducing saturated steam into heated asphalt through a specially designed nozzle. The reduced viscosity increased the volume and reduced the surface energy in the foamed-asphalt allowing intimate coating when mixed with the cold, wet aggregate [2]. In 1968, Mobil Oil Australia modified the original process by adding cold water rather than steam in the hot bitumen. This method made the asphalt foaming process much more practical and less expensive. The benefits of foamed-asphalt stabilization as summarized by Nataatmadja include: (a) an increase in strength over unbound materials, (b) a quick construction method, (c) lower cost than reconstruction, (d) immediate trafficking, and (e) improved durability and material resistance to moisture infiltration [3].

Researchers reported that the amount of fines (percentage of aggregate material passing the No. 200 sieve) and asphalt content are considered to be the most important factors in a foamed-asphalt mixture design [1], [4], [5]. A minimum of 3 percent passing the 0.075 mm (No. 200) sieve is considered as a basic requirement to obtain a promising foamed-asphalt mixture. Because asphalt tends to coat the fines and partly coat the larger articles, Lee also suggested an upper limit of the percentage passing the No. 200 sieve in the range of 35 and 40 percent [5]. Csanyi suggested that the proper amount of water for any mix might be determined by a few trial batches [1]. For foamed-asphalt treated soil, researchers

recommended that the optimum water content should be the moisture content at which the soil aggregate has its maximum bulk volume *[4]*, *[6]*.

As with any asphalt-aggregate mixture, the structural properties of foamed-asphalt mixtures are dependent on the asphalt content *[7]*, *[8]*. Bowering et al. found that mixtures made with foamed-asphalt and with asphalt emulsion had similar properties up to an asphalt content of 1.5 percent by dry weight of aggregate *[3]*. Above this level of asphalt content the foamed-asphalt mixtures displayed improved structural properties. Curing of foamed-asphalt mixtures occurs as the water evaporates with time. Studies demonstrate the feasibility of using salvaged material to produce a foamed, recycled mixture with or without virgin materials *[2]*, *[5]*, *[9]*, *[10]*. Generally, the mixture properties were improved when fines were added to the recycled materials.

In a 2003 rehabilitation project on US 190 near Baton Rouge, an experimental foamed-asphalt base was constructed using the Wirtgen foamed-asphalt process *[11]*. The continuously reinforced concrete pavement design called for a lime-treated subbase and 8 in. of stone base. Two experimental foamed-asphalt base sections, each 1000 ft. long and 8 in. thick, were constructed on this project. One foamed-asphalt base contained 100 percent RAP materials and the other used the combination of 75 percent RAP and 25 percent crushed concrete. Initial laboratory testing results indicated that the foamed-asphalt treated bases increased both cohesion and triaxial strength *[12]*. Furthermore, non-destructive tests during construction indicated that the foamed-asphalt treated recycled materials showed higher in-situ stiffness values and structural numbers than those of a lime stone base layer. However, the long-term performance of this type of base material was unknown, especially due to the presence of moisture and other environmental effects, such as aging.

The Maine Department of Transportation (MaineDOT) recently published a report on using foamed-asphalt as a stabilizing agent in a full depth reclamation project *[13]*. Based on five-year performance results (i.e., rut depth, cracking, IRI, and structural number), it was concluded that a section containing 3-in. hot mix asphalt (HMA) and 8-in. foamed-asphalt stabilized full-depth reclamation base ("foamed section") performed slightly better than a section with 4-in. HMA and a full-depth reclamation base without foamed-asphalt treatment ("regular section"). The cracking data also showed that the "foamed section" had a significantly less amount of cracking than the "regular section" during the first four years. However, the transverse, longitudinal, and load cracking on the "foamed section" increased to about the same level as the "regular section" on the fifth year. The reason for the rapid

increase in cracking in the fifth year in the foamed-asphalt section was not investigated. Therefore, the long-term performance of foamed-asphalt materials is still uncertain.

A failure investigation on a warranty project in Texas concluded that the cause for a premature pavement failure due to extensive surface distresses (e.g., rutting and cracking) could be directly related to the moisture susceptibility of the foamed-asphalt base materials used *[14]*. A failure hypothesis resulted from that study is presented in Figure 1. The water was assumed to enter the base materials due to the suction action from a wet subgrade. Basically, the strength of the foamed-asphalt base continues to decrease with moisture, and eventually there is no sufficient strength to withstand traffic loading, which led to total structural failure, Figure 1.
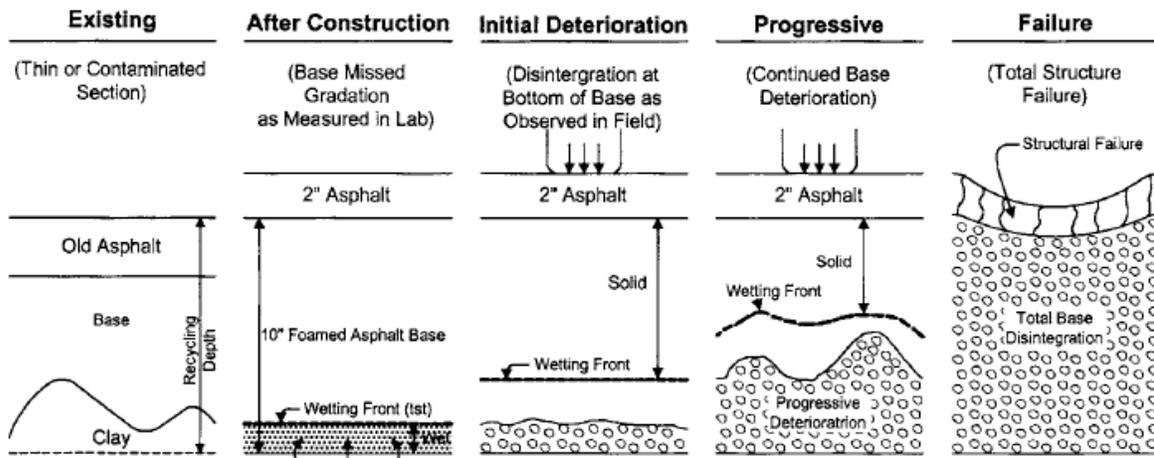
Figure 1
Failure mechanism of foamed-asphalt pavements *[14]*

OBJECTIVE

The objective of this study was to evaluate the field performance of foamed-asphalt treated RAP base materials as compared to a conventional crushed stone base under accelerated loading.

SCOPE

Three full-scale APT test sections were evaluated in this study. It included field instrumentation for monitoring ALF load induced pavement responses, non-destructive testing, surface distress surveys, and the evaluation of pavement structural performance of the test sections. In addition, a series of laboratory engineering performance-based tests including resilient modulus, permanent deformation, and loaded wheel tracking (LWT) were performed to characterize the performance of utilized materials in the APT experiment.

METHODOLOGY

Description of APT Test Sections

Pavement Structures

Figure 2 presents the pavement structures for the three APT test sections considered in this study. Each APT section was 13 ft. wide by 107.5 ft. long. As shown in Figure 2, each section included a 2.0-in. HMA wearing course, an 8.5-in. base course, and a 12-in. cement-treated working table layer over an A-4 embankment subgrade. All section designs were identical except for the base layers. The base courses for sections 4-2B, 4-3A, and 4-3B were crushed stone, a foamed-asphalt treated base of a blend of 50 percent RAP and 50 percent recycled soil cement, and a foamed-asphalt treated base of 100 percent RAP, respectively. Also outlined in Figure 2 is the field instrumentation layout on each test section, which will be discussed in a subsequent section.
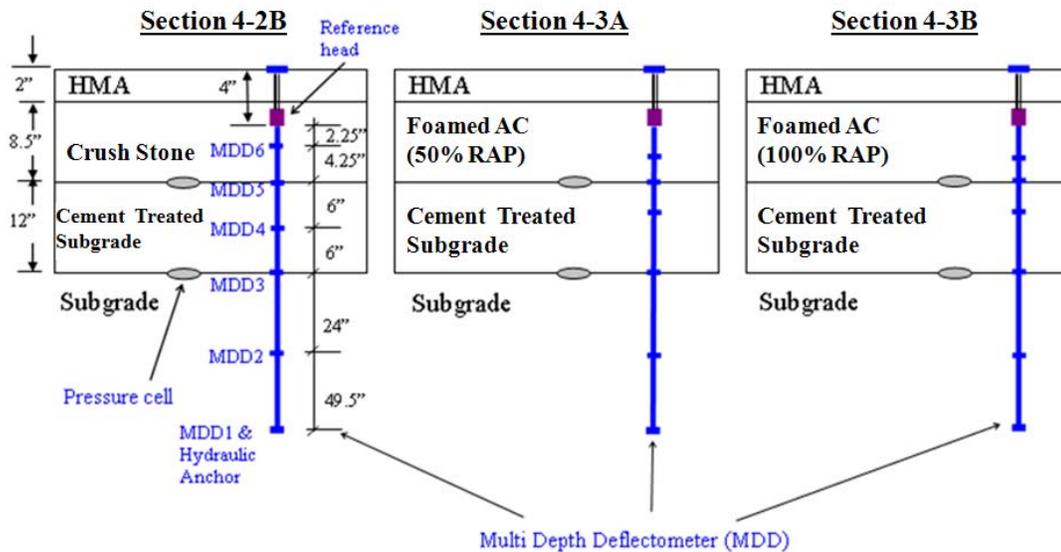
Figure 2
Pavement structures of ALF test sections

Materials

Wearing Course HMA Mixture. A ¾-in. Superpave HMA mixture, designed at a compaction effort of 100 gyrations, was used in the wearing course layer. Table 1 presents the job mix formula. The aggregate blend consisted of 45.4 percent No. 67 coarse granite aggregate, 17.1 percent No.11 crushed siliceous limestone, 10.3 percent coarse sand, 12.9

percent crushed gravel, and 14.3 percent RAP. The binder type selected was an elastomeric polymer-modified type meeting Louisiana PG specifications of PG76-22M for high-volume traffic mixtures *[15]*. The optimum asphalt binder content was 4.4 percent, including 0.7 percent of aged asphalt cement from RAP *[16]*.

Table 1
Job mix formula

Wearing Course HMA	
Binder Type	PG76-22M
Design Binder content, %	4.4
%G_{mm} at N_I	88.4
%G_{mm} at N_D	96.1
%G_{mm} at N_M	96.8
Design air voids, %	3.9
VMA, %	13.8
VFA, %	71.0
US Sieve	**Percent passing**
1 in.	100
3/4 in.	97
1/2 in.	83
3/8 in.	73
No. 4	49
No. 8	33
No. 16	24
No. 30	18
No. 50	10
No. 100	5.7
No. 200	4.6

Base Materials. The foamed-asphalt treated base materials used in this experiment were designed by McAsphalt Engineering Services in Scarborough, ON, Canada, and constructed using a Wirtgen WR 2500 S mixing machine. In particular, the base material used in section 4-3A was a foamed-asphalt treated blend of 50 percent RAP and 50 percent recycled soil cement (hereafter called as FA/50RAP/50SC), and the base for section 4-3B was a foamed-asphalt treated 100 percent RAP (hereafter called FA/100RAP). Table 2 presents a summary report of design data for the two foamed-asphalt base materials. Note that a PG58-22 binder was used in the foaming process with a design binder content of 2.8 percent and 2.5 percent for the FA/ 50RAP/50SC and FA/100RAP, respectively. Also shown in Table 2, high percentages of air voids were designed and both foamed-asphalt treated materials seemed to possess relatively low strength values from the indirect tensile strength (ITS) test conducted. The RAP material used in the base treatment was obtained from the contactor's stockpile. The gradation and physical properties for the RAP material are

presented in Table 3. Note that 1.5 percent lime and 1 percent cement were added to FA/50RAP/50SC and FA/100RAP mixtures, respectively, during the construction. More details can be referred to elsewhere *[17]*.

Table 2
Design data for foamed-asphalt RAP

Property	FA/100RAP	FA/50RAP/50SC
Asphalt Cement Type	PG58-22	PG58-22
Design Asphalt Cement (%)	2.5	2.8
Indirect tensile strength (ITS) - Dry, psi	53.0	46.7
ITS - Wet, psi	50.0	38.4
Retained ITS (%)	94.5	82.4
Selected moisture content	6	8
Bulk Relative Density (lb/ft^3)	124.8	117.3
Air Voids (%)	15.3	20.3

Table 3
Properties of RAP base materials

US Sieve No.	Percent Passing
2.5 in	100
2 in	100
1.5 in	100
1 in	100
¾ in	100
½ in	97
3/8 in	87
No. 4	65
No. 8	51
No. 16	42
No. 30	35
No. 50	22
No. 200	9
Laboratory Physical Properties	
Optimum water content (%)	8.6
Max. dry unit weight (kN/m^3)	18.6
AASHTO soil classification	A-1-a
Unified soil classification system (USCS)	GP

The stone base course of section 4-2B was a crushed limestone base, designed as Class-II base course specified by LADOTD's standard specifications for roads and bridges *[15]*. The specified gradation requirements for a Class-II stone base are listed in Table 4. Note that the specification also requires that the maximum liquid limit and the maximum plasticity index shall be less than 25 and 4 percent, respectively, for the fraction of stone passing the No. 40 sieve *[15]*.

Table 4
Gradation and specification requirements for Class-II stone base

U.S. Sieve	Specification	Percent Passing
1½ in.	100	100
1 in.	90~100	97
¾ in.	70~100	88
½ in		74
3/8 in		67
No. 4	35~65	50
No. 8		36
No.16		26
No. 30		20
No. 40	12~32	n/a
No. 50		15
No.200	5~12	11

Subbase Materials. The subbase course designed for this experiment was in-place cement treated soils with an 8 percent cement content by volume. The soil used in the subbase treatment was a silty clay embankment soil with a plastic index (PI) of 10. Table 5 presents the basic soil properties. More details about the cement treated soil subbase can be found elsewhere *[16]*.

Table 5
Soil properties

Passing # 200 (%)	Clay (%)	Silt (%)	LL(%)	PI	W_{opt} (%)	γ (kN/m³)	Classification	
							USCS	AASHTO
91	23.5	60.3	31	10	18.5	17.1	CL-ML	A-6

Instrumentation. Field instrumentation of the APT experiment consisted of using multi-depth deflectometers (MDD) and earth pressure cells for measuring load-induced vertical deformations and compressive stresses. The instrumentation layout is shown in Figure 2. For each test section, two Geokon 3500 pressure cells were embedded at two depths directly along the centerline: one at the bottom of the base layer and the other on top of the subgrade. One MDD with six potentiometers (deformation measurement sensors) was installed on each test section at a distance of 4.5 ft. away from the pressure cell location along the centerline. More details on instrumentation devices can be found elsewhere *[17]*.

Laboratory Material Characterization

As part of the APT experiment, a suite of mechanistic and simulative tests were performed to evaluate the lab performance of the wearing course HMA mixture and different base materials under various loading and environmental conditions. It should be noted that laboratory tests performed on the cement treated subbase and the embankment soils have been reported elsewhere *[16]*.

Characterization of HMA Mixture

Sufficient plant-mixed loose HMA mix as well as field cores were collected and used to prepare laboratory testing specimens for different mechanistic tests. Table 6 presents testing temperatures and protocols for each HMA test considered in this study. Detailed descriptions of HMA tests are presented in the Appendix of this report.

Table 6
Laboratory tests performed on HMA mixtures

Mixture Properties	Laboratory Tests	Test Temperature	Test Protocol
Viscoelastic properties of HMA mixtures	Dynamic Modulus Test (E* and ϕ)	-10ºC – 54.4ºC	AASHTO TP62-03
Permanent deformation	Flow Number Test (F_N)	Effective Pavement Temperature (T_{eff})	NCHRP Project 9-19
Moisture sensitivity and permanent deformation	LWT (Hamburg)	122 º F (50ºC)	AASHTO T 324-04
Tensile Strength and Strain	Indirect Tensile Strength (ITS)	77º F (25°C)	AASHTO T245
Fatigue / Fracture	Semi-circular bending (SCB) test	77º F (25°C)	*[18]*
Permanent deformation	Asphalt Pavement Analyzer (APA)	High Temperature of the Superpave Binder PG Grade	AASHTO TP 63
Dynamic Shear Modulus and Shear Phase Angle	Frequency Sweep Test at Constant Height (FSCH)	-50°F – 130°F (-10ºC – 54.4ºC)	AASHTO TP7

Characterization of Base Materials

Resilient modulus and permanent deformation laboratory tests were performed to characterize the resilient and permanent deformation behavior of the crushed stone and foam

asphalt treated RAP base materials used in the ALF experiment. The tests were conducted on cylinder samples with a diameter of 6 in. and a height of 12 in. All samples were remolded from material collected in the field and compacted in the laboratory at their in-situ moisture condition. In addition to capture rutting performance under a submerged moisture condition, the Hamburg wheel tracking and Asphalt Pavement Analyzer (APA) tests included in the preceding HMA section were conducted on slab samples fabricated from the foamed-asphalt treated base materials used in this experiment. The Hamburg type wheel tracking test was conducted at a temperature of 104° F, while the Asphalt Pavement Analyzer test was conducted at two temperatures: 104° F and 122° F.

Resilient Modulus Tests. The resilient behavior of base materials is usually characterized by the resilient modulus, which is typically determined in laboratory repeated loading triaxial (RLT) tests. The RLT tests used to determine resilient modulus in this study was performed in accordance with AASHTO-T307 *[19]*. In this method, a series of steps consisting of different levels of cyclic deviatoric stress are followed. The cyclic loading consists of repeated cycles of a haversine shaped load-pulse of a 0.1-sec. load duration and 0.9-sec. rest period. It is noted that all resilient modulus RLT tests were conducted using the Material Testing System (MTS) 810 machine with a closed loop servo-hydraulic loading system, shown in Figure 3.

In order to determine the resilient modulus parameters of the base materials, the average value of the resilient modulus for each stress sequence was first calculated. A regression analysis was then conducted to fit test data to the generalized constitutive model adopted by the new Mechanistic-Empirical Design Guide shown in the following equation *[20]*:

$$M_R = p_a k_1 \left(\frac{\theta}{p_a} \right)^{k_2} \left(\frac{\tau_{oct}}{p_a} + 1 \right)^{k_3} \tag{1}$$

where,
M_R = the resilient modulus;
Pa = the atmospheric pressure (14.7 psi);
$\theta = (\sigma_1 + \sigma_2 + \sigma_3)$;
σ1, σ2, σ3 = principal stress components;
τ_{oct} = the octahedral shear stress, which is a measure of the distortional (shear)
      stress on the material, and is defined as:

$$\tau_{\text{oct}} = \frac{1}{3}\sqrt{(\sigma_1 - \sigma_2)^2 + (\sigma_1 - \sigma_3)^2 + (\sigma_2 - \sigma_3)^2} \text{ ; and}$$

k_1, k_2, and k_3= the material parameters.

Figure 3
RLT test setup

Permanent Deformation Test. The permanent deformation test is also an RLT test. The test consists of conditioning the samples in the same procedure used in the resilient modulus tests. This is followed by applying 10,000 load cycles at a constant confining pressure of 5 psi and a peak cyclic stress of 15 psi. These stress levels were selected based on a stress analysis conducted to compute a field representative stress condition in the base layer. Tests were stopped after 10,000 load cycles or when the sample reached a permanent vertical strain of 7 percent, whichever occurs first. Each cycle consisted of the same load pulse used in resilient modulus tests. During the permanent deformation repeated load triaxial test, at pre-set intervals of loading, vertical deformation was continuously recorded. Figure 4 presents the permanent (plastic) strain (ε_{pn}), resilient strain (ε_r), total strain (ε_{tn}), and resilient modulus obtained for a typical load cycle determined from the test results.
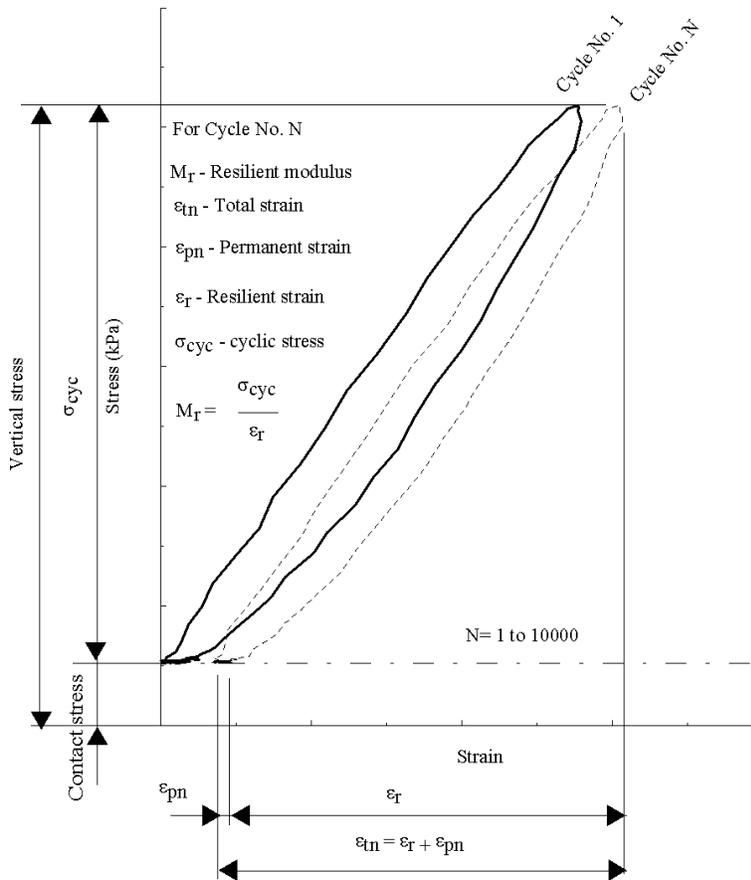
Figure 4
Stress and strain cycles used in the permanent deformation test

Accelerated Loading Experiment

ALF Loading History

The APT loading device used is called the ALF (Accelerated Load Facility). The three APT test sections included in this study were part of the fourth ALF experiment at LTRC. The entire APT loading period of ALF 4 was divided into two testing phases: the first phase was designated for testing three "A" sections; whereas, the second phase was for loading three "B" sections. Thus, section 4-3A was tested during the first testing phase and both sections 4-2B and 4-3B were completed during the second. Each testing phase lasted approximately one year. To expedite traffic-induced pavement deteriorations, two steel load plates of 2,300-lb. each were added to the

Table 7
ALF loading history

Section	No. of Passes (x 1000)	Total Load lb. (kN)	ESAL Factor	ESALs	Cumulative ESALs
4-2B	0 - 175	9,750 (43)	1.377	241,039	241,039
	175 - 225	12,050 (53.6)	3.213	80,338	355,811
	225 - 300	14,350 (63.6)	6.463	484,729	840,540
4-3A	0 - 175	9,750 (43.0)	1.377	241,039	241,039
	175 - 225	12,050 (53.6)	3.213	160,674	401,713
4-3B	0 - 175	9,750 (43.0)	1.377	241,039	241,039
	175 - 225	12,050 (53.6)	3.213	80,338	355,811
	225 - 300	14,350 (63.6)	6.463	484,729	840,540

ALF load assembly (with a self-weight of 9,750-lb.) specifically at the loading cycle numbers of 175,000 and 225,000, respectively. The loading history on the three sections is presented in Table 7 with converted 18,000-lb. equivalent single axial load (ESAL) numbers. Note that the testing on section 4-3A stopped earlier than the other two sections due to an early pavement structure failure.

Failure Criteria

For this experiment the failure parameters were set forth by the research team. A test section was considered to have failed when the pavement condition meets one of the following failure criteria, whichever comes first: (1) an average rut depth of 0.5-in among eight measurement stations within the trafficked area of a section; or (2) 50 percent of the trafficked area of a section develops visible cracks (e.g., longitudinal, transverse, and alligator cracks) more than 1.5 ft/ft^2.

Field Measurements

The field instrumentation data including the MDD and pressure cell readings were collected at approximately every 8,500 ALF load repetitions. All pavement responses were measured under the left tire of the ALF dual tire assembly when the tire was directly positioned on the top of an instrumentation device (i.e., pressure cell and MDD).

NDT tests including the Dynaflect and falling weight deflectometer (FWD) as well as the rutting and cracking survey were performed at the end of each 25,000 load repetitions. The effective loading area of ALF testing is about 32 ft. long in which deflection measurements and distress survey were taken at 8 stations at 4-ft. intervals. More details on NDT tests and distress surveys can be referred to elsewhere *[17]*.

Data Analysis Techniques

The data analysis included the processing of NDT deflection data, evaluation of instrumentation results, modeling pavement structure, and the prediction of pavement performance in terms of pavement distresses. The following analysis procedures and software were used in this study.

Dynaflect-Deflection Based Pavement Evaluation Chart

Kinchen and Temple developed a Louisiana pavement evaluation chart for the estimation of existing pavements' structural numbers based on Dynaflect measured deflection *[21]*. As shown in Figure 5, an effective structural number and a design subgrade modulus of existing pavements can be determined based on a temperature-corrected Dynaflect center deflection and a percent spread value. The percent spread (*Sp*) is the average deflection of the central deflection in a percentage:

$$Sp = \frac{D_0 + D_{300} + D_{600} + D_{900} + D_{1200}}{5 \times D_0} \times 100 \, percent \qquad (2)$$

where,
D_{300}, D_{600}, D_{900}, and D_{1200} = deflections measured at 12 in., 24 in., 36 in., and 48 in. from the center of the applied load.

This method was used in the analysis of Dynaflect deflection results for determining test section's effective structural number under different ALF repetitions.
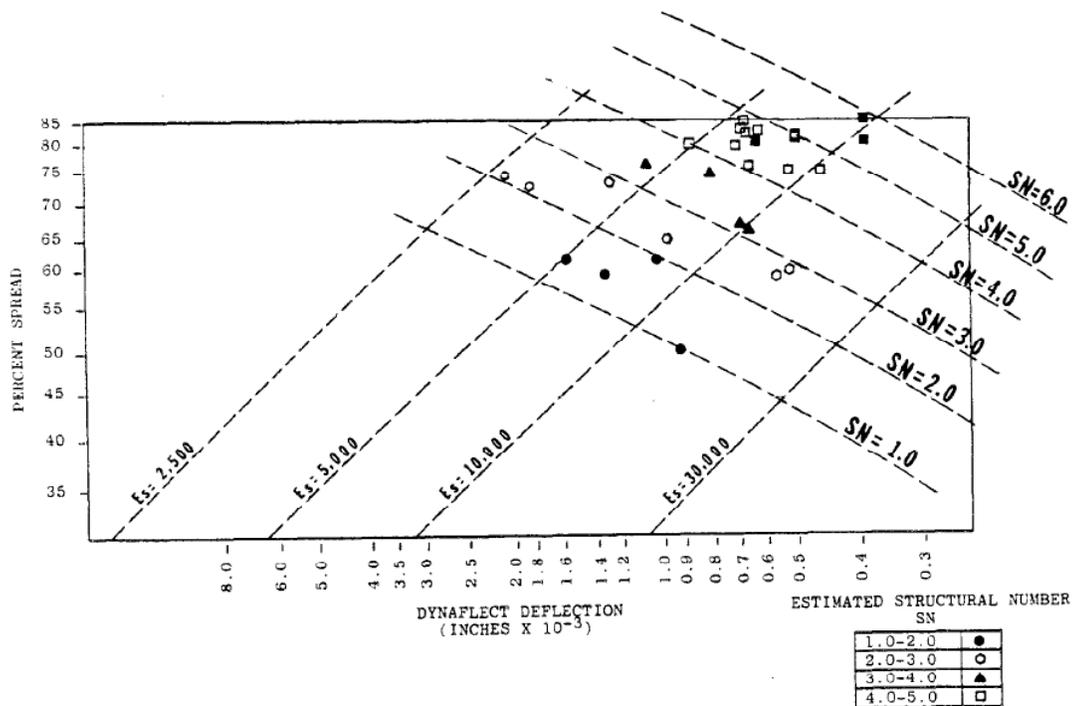
Figure 5
Louisiana pavement evaluation chart *[21]*

EVERCALC

EVERCALC is a windows-based computer program developed by the Washington DOT for backcalculation of layer moduli based on FWD measured deflection basins *[22]*. EVERCALC is based on the multilayered elastic analysis program, WESLEA (provided by the Waterways Experiment Station, U.S. Army Corps of Engineers), which produces pavement response parameters, such as stresses, strains, and deformations in the pavement system. EVERCALC was used in this study for the backcalculation of layer moduli based on FWD measured deflection bowls.

During the backcalculation process, primarily due to the very thin asphalt top layer (2 in.) used in pavement test sections, it was found that directly using a four-layer pavement structure as shown in Figure 2 could not back calculate a set of reasonable modulus values based on the FWD deflection bowls measured. In fact, very large root mean square (RMS) errors were observed on trials of many FWD deflections. In addition, the EVERCALC program tends to provide a very high modulus value (generally higher than 290 ksi) for the lime treated soil layer used in test sections. The modulus value of 290 ksi is significantly higher than those obtained in laboratory testing on this type of material (a range from 25 to 50 ksi). In order to obtain a relatively realistic set(s) of layer modulus for base and other

materials, the elastic modulus of the HMA layer was set to a fixed value of 725 ksi at 68 °F in all FWD backcalculations.

Performance Prediction using VESYS

A VESYS 5W computer program –windows version of VESYS 5–was employed in this study to predict the rutting development of ALF test lanes *[23], [24]*. The basic assumption used in the VESYS rutting prediction model is that permanent strain developed in each pavement layer is a linear function of its elastic strain under the load, which is expressed in the following equation:

$$\Delta\varepsilon_\text{p}(\text{N}) = \varepsilon_\text{e} \times \mu \times \text{N}^{-\alpha} \tag{3}$$

where,

$\Delta\varepsilon_\text{p}$ = Permanent strain per load repetition,

ε_e = Dynamic resilient strain,

α, μ = Material permanent deformation parameters, and

N   = Number of load repetitions.

Three category types of inputs: climate inputs, structure & materials property, and traffic are required in the VESYS 5W computer program. A brief description of each category is provided below.

    Climate Inputs. Required data are number of seasons, season length, and moisture effect factor. In this study, nine seasons were chosen in the analysis. Each of the first seven seasons was assigned to have 40 days in which 25,000 ALF passes were assumed to apply to the pavement. The last two seasons, each having 42.5 days, were assumed to have higher daily load repetitions for simulating the ALF load with an additional load plate. The default temperature data for the Louisiana "South Zone" provided in the VESYS program was used. The moisture effect factor was set to be 1.0 since the layer modulus of individual layers was provided for each of nine analysis periods.

    Structural & Material Properties. In the rutting prediction, the default inputs for a rut resistant HMA mixture included in the program were chosen for the 2-in. HMA layers. Similarly, default inputs were considered for subbase and subgrade materials in the analysis. However, laboratory permanent deformation results were used to compute the required permanent deformation inputs, of GNU (μ) and ALPHA (α) for three base materials considered. This is because the VESYS analysis was primarily aimed to assess the

performance of various base materials. The following equations were used in the determination of those input parameters from permanent deformation test results (described in the next section):

$$\mu = ab/\varepsilon_r \qquad (4)$$

$$\alpha = 1-b \qquad (5)$$

where,

a, b = regression parameters from the permanent deformation curve; and

ε_r = resilient strain at 200th load repetitions.

Table 8 presents the VESYS permanent deformation parameters determined from the permanent deformation test results for the three base materials considered. The details of permanent deformation tests conducted in this study will be described in the next section.

Table 8
VESYS permanent deformation parameters

Material	$\varepsilon_r@$ 200cycles (x10-6)	a	b	μ	α
Crushed Stone	437	0.017	0.31	0.121	0.69
FA/50RAP	503	0.0112	0.42	0.094	0.58
FA/100RAP	570	0.0145	0.45	0.14	0.55

Traffic. The "Advanced input" option was used to simulate the ALF loading sequence of this experiment. The simulated wheel load was 9,750 lb. with a tire pressure of 105 psi. In the first seven seasons, the daily loading repetitions was set to be 625; for the last two seasons the daily repetition was assumed to be 1373. Such traffic input would provide a total of 291,650 load repetitions of the 9,750-lb. load to simulate the total 225,000 ALF passes with the first 175,000 repetitions of 9,750 lb. and the last 50,000 repetitions of 12,050 lb.

DISCUSSION OF RESULTS

Results presented for discussion included those from laboratory tests, field non-destructive deflection measurements, instrument responses to vehicular loading, surface distress surveys, and forensic investigation on failed pavement structures. In addition, pavement rutting performance was analyzed using the newly developed MEPDG software, and the structural layer coefficients for the two chemically stabilized BCS base materials used in this study were quantitatively estimated based on the APT performance results.

Laboratory Test Results

Test Results for HMA Mixture

The stiffness properties of the HMA mixture were evaluated using the dynamic modulus test. Two parameters were obtained from this test, the dynamic modulus (E*) and the phase angle. Figure 6 shows the isotherms of the average dynamic modulus values at different temperatures and frequencies. By comparing the obtained E* values with those catalog dynamic modulus values of Louisiana HMA mixtures, it was noted that the considered HMA mixture had similar dynamic modulus values as those for ¾-in nominal maximum size (NMS) Superpave mixtures used in the construction of medium traffic highways in Louisiana *[25]*. The variation of the phase angles with the dynamic modulus is shown in Figure 7 for the tested HMA mixture. This figure can be used to illustrate the phase angle response to frequency. The phase angle increased with increasing frequency, reached a peak, and then decreased. This response is different from the asphalt binder in that the phase angle for an asphalt binder generally decreases with increasing frequency. The reason for this is that, at high frequency (low temperature), the asphalt binder primarily affects the phase angle of asphalt mixtures, i.e., binder viscoelastic follows similar trend. However, at low frequency (high temperature), it is predominantly affected by the aggregate, and therefore, the phase angle for asphalt mixture decreases with decreasing frequency or increasing temperature because of the aggregate influence.

As described in Table 6, several other fundamental engineering tests were also conducted to examine the laboratory performance of the HMA mixture used in the APT test sections at high, intermediate, and low temperatures. In general, the results of tests conducted at high temperatures (LWT, FSCH, and E* tests) indicated that the HMA mixture had a rutting resistance similar to those obtained for well-performing Superpave mixtures in the state of Louisiana. Furthermore, the SCB, ITS, E* showed that this mixture had good fatigue

cracking resistance at intermediate and low temperatures. More detailed laboratory results for the HMA mixture can be found in the Appendix of this report.
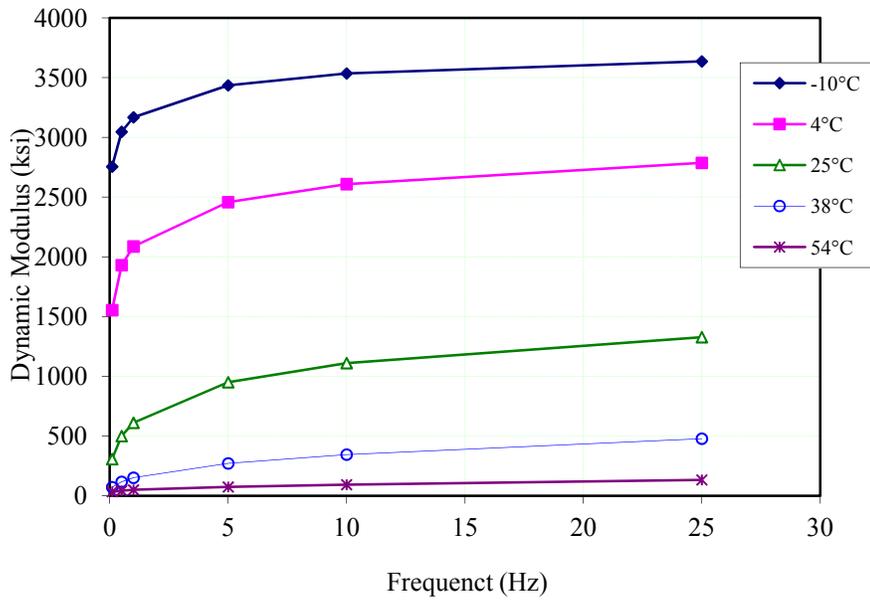
Figure 6
Dynamic modulus test results – HMA mixture
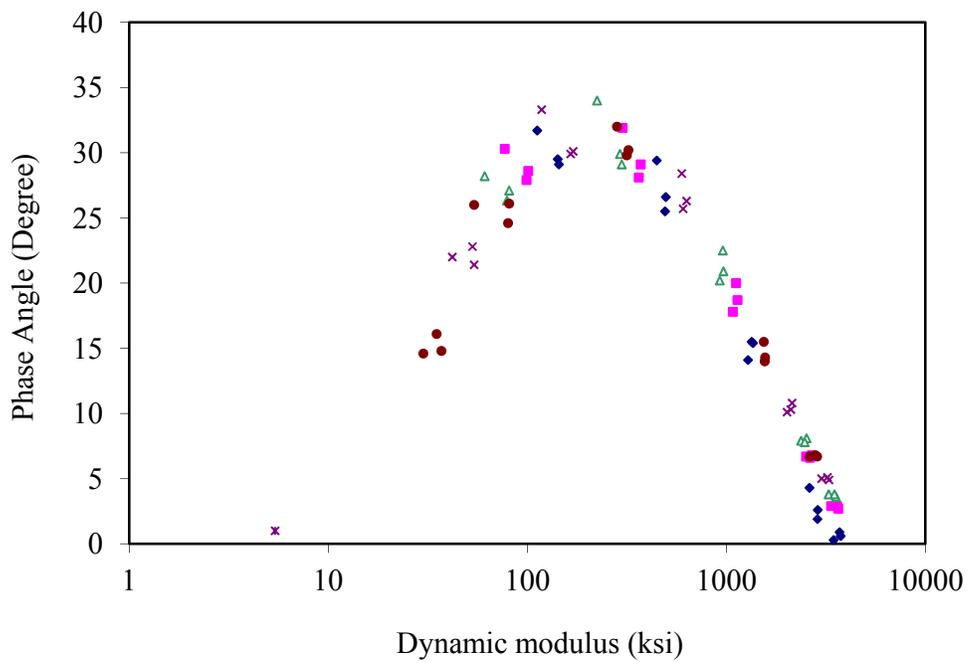
Figure 7
Variation of phase angles with dynamic modulus – HMA mixture

Test Results of Base Materials

Resilient Modulus Test. Figures 8-10 present the variation of the M_r with bulk stress (σ_b) and confining stress (σ_c) of the crushed stone, FA/100RAP, and FA/50RAP/50SC base materials, respectively. As shown in Figure 8, the M_r of crushed stone increased with the increasing of either σ_b or σ_c. This observation was because an increase in the σ_b would increase frictional resistance among crushed stone particles and an increase of σ_c would decrease material dilatational properties. On the other hand, it was noted from Figures 9 and 10 that, in general, the two foamed-asphalt treated RAP materials had similar resilient properties in terms of M_r. At a constant confining stress, the M_r of both foamed-asphalt treated RAP materials decreased as the σ_b increased. This may be attributed to the decrease in friction among the foamed-asphalt treated RAP particles because of the smooth asphalt coating around them. However, as the confining pressure increases, the M_r of foamed-asphalt treated RAP increases. Such a behavior is similar to that of a crushed stone. Overall, the evaluated crushed stone material showed higher M_r values than the foamed-asphalt treated RAP materials, especially under high σ_b levels.
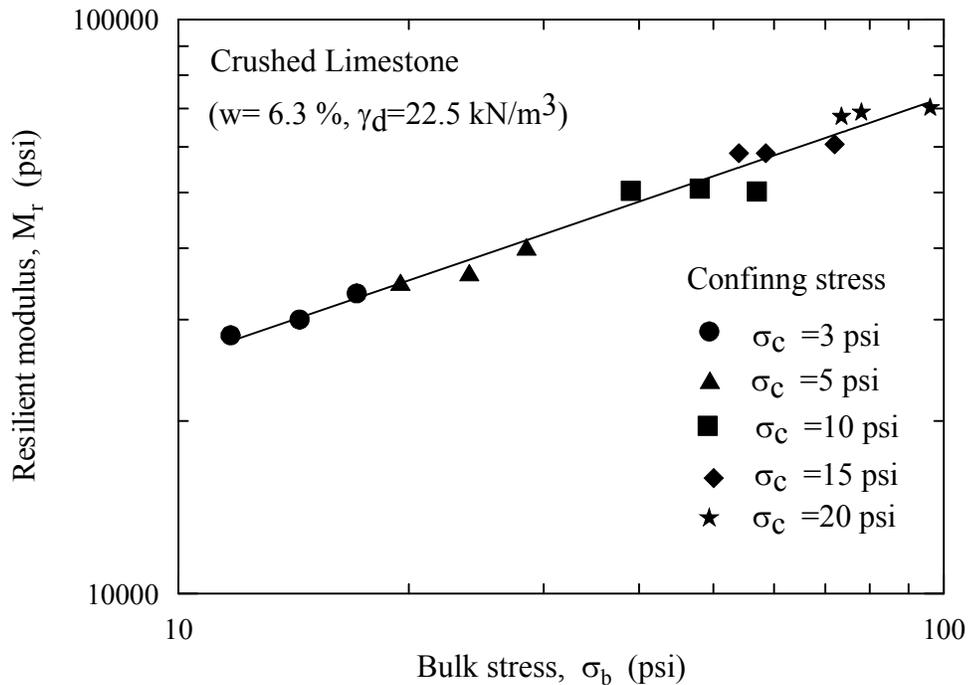
Figure 8
Resilient modulus of crushed stone base
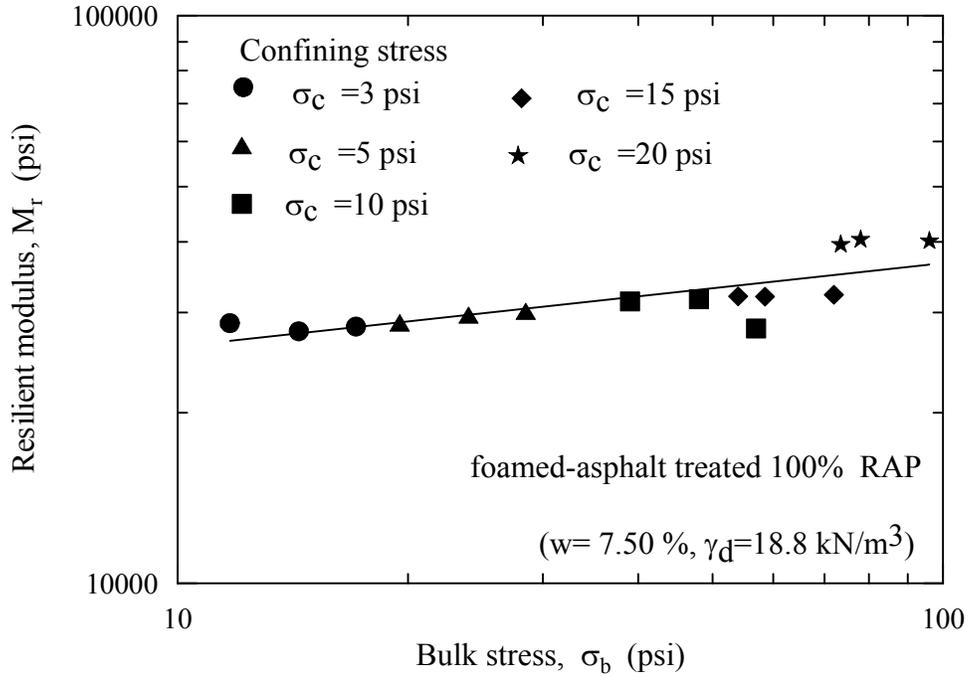
Figure 9
Resilient modulus of FA/100 RAP base
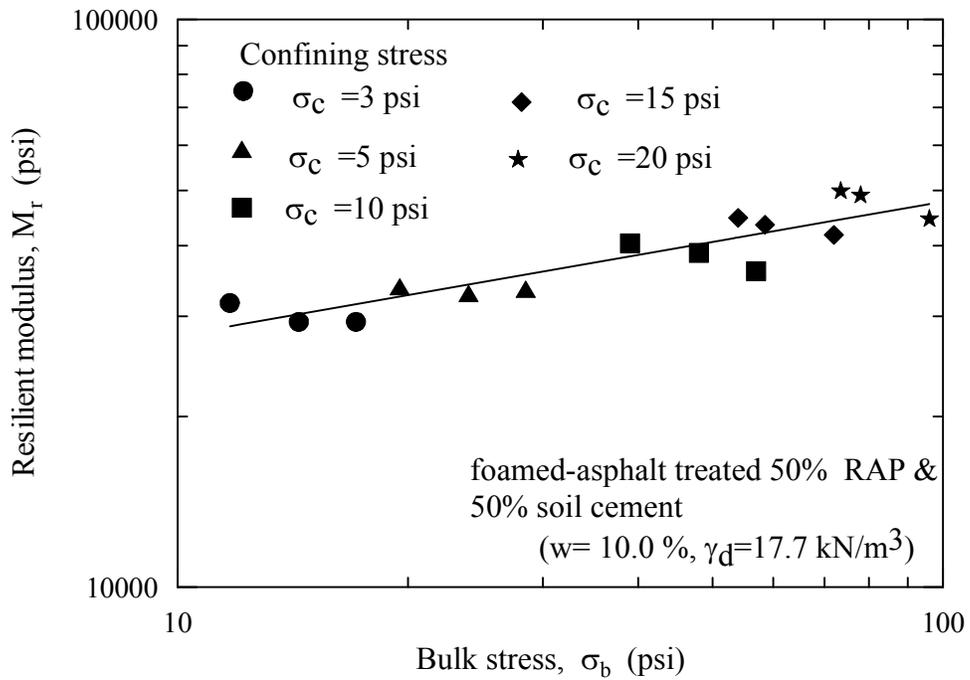
Figure 10
Resilient modulus of the FA/50RAP/50SC base

Permanent Deformation Test. The permanent deformation test acquired loads and vertical deformations continuously throughout the 10,000 cycles. The total strain, resilient strain, permanent strain, and resilient modulus for each load cycle were then computed. The permanent strain curves of crushed stone and foamed-asphalt RAP materials tested in this study are shown in Figure 11. The crushed stone material exhibited an initial accelerated rate of permanent strain with the increase of load repetitions and then reached a steady state, while the FA/50RAP/50SC accumulated slightly higher permanent strain than the crushed stone material. Furthermore, the permanent strain curve with the number of load cycles of FA/100RAP increased at an accelerated rate without showing any steady state. It is noted that the foamed-asphalt treated 100 percent RAP accumulated the largest permanent strain among all the base materials evaluated, followed by foamed-asphalt treated 50 percent RAP with 50 percent soil cement. The permanent deformation resistance properties under repeated loading degraded in the foamed asphalt RAP base.
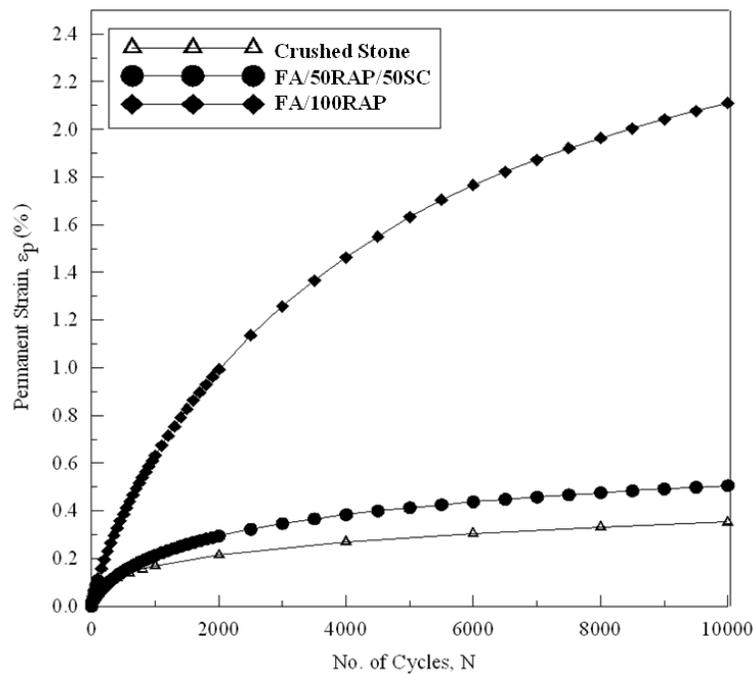
Figure 11
Permanent strain curves for RAP materials

The permanent strain curve obtained from repeated loading triaxial test results was also fitted to a model that used the following function:

$$\varepsilon_p = aN^b \tag{6}$$

where,

ε_p = cumulative permanent strain (%),

N = number of load cycles, and

a and b = material parameters.

Table 9 presents the material parameters estimated from the power function used for each base material considered. Low values of intercept (a) and slope (b) are desirable for better rut resistance of base layers. It is noted that, in general, the fitted permanent strain curve of the crushed stone material had higher intercept (the "a" value) but lower slope (the "b" value) compared to other foamed-asphalt treated RAP materials. This indicates that initially the crushed stone material accumulated higher permanent strain; however, the rate of the accumulation during the test was lower. This suggests that the crushed stone exhibited better permanent deformation resistance compared to the foamed-asphalt treated RAP materials considered in this study.

Table 9
Permanent strain model parameters and strains of base materials

Material	Model Parameters		
	a	b	R^2
Crushed Stone	0.016300	0.34	0.999
FA/50RAP/50SC	0.011200	0.42	0.990
FA/100RAP	0.014500	0.55	0.990

Legend: a and b- Permanent strain model parameters, R^2- Coefficient of determination, ε_r - Resilient strain (percent), ε_p - Cumulative permanent strain (percent), and ε_t - Cumulative total strain (percent)

Loaded Wheel Tracking Test. The Hamburg Type Wheel Tracking test and Asphalt Pavement Analyzer were conducted on the foamed-asphalt treated RAP materials to evaluate its performance under severe load and environmental conditions. Figure 12 presents the average rut depths obtained from the results of those tests. It is noted that foamed-asphalt treated RAP materials rut depth increased with increasing the temperature. Furthermore, at the same testing temperature, the considered foamed-asphalt treated RAP materials accumulated a much higher rut depth under the wet condition in the Hamburg Type Wheel Tracking test compared to the dry condition in the Asphalt Pavement Analyzer test. This indicates that those materials exhibit high moisture susceptibility.   Finally, it was noted that the FA/50RAP/50SC material exhibited a greater moisture susceptibility than FA/100RAP material.
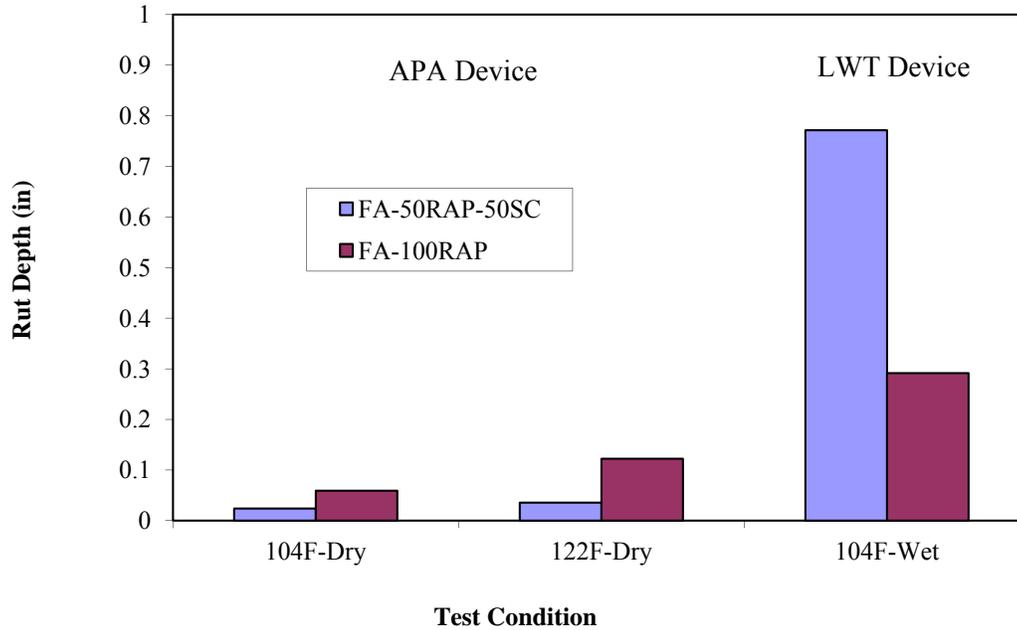
Figure 12
Results of loaded wheel tracking tests

Accelerated Pavement Testing Results

ALF Loading Results

Figures 13-15 show pavement surface photos of each APT test section at the failure. All sections had developed significant surface rutting. The ALF loading was stopped on an APT test section when average rut depths were greater than 0.5-in. deep. Some severe localized fatigue cracks were observed on all sections at the end of ALF loading. The localized cracks were directly resulted from the large surface depression (or rutting) developed in those areas. According to the failure criteria set by this experiment, all three test sections had a rutting failure (i.e. reaching the rutting limit before cracking criterion was met).

In addition, it was noticed several months after construction, small droplets of asphalt binder material started to seep up through the surface of the FA/100RAP test section (4-3B) and these asphalt droplets became much more noticeable as the load repetitions increased, as shown in Figure 15. It should be also noted that the dark surface shown on the loading area

Figure 13
Failure surface of stone base section (4-2B)

>1"
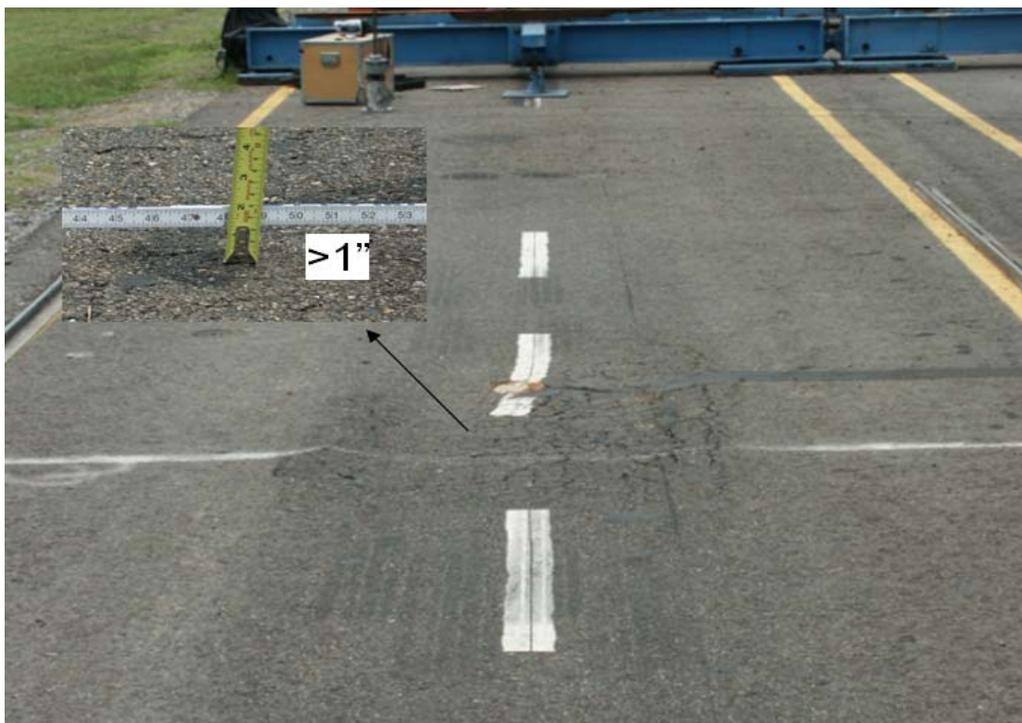
Figure 14
Failure surface of FA/50RAP/50SC section (4-3A)

Figure 15
Failure surface of FA/100RAP section (4-3B)

of section 4-2B (Figure 13) was the color of asphalt droplet material of section 4-3B, which first stuck to the ALF dual tires and then printed on the surface of section 4-2B during the alternative ALF loading.

Figure 16 presents the mean measured rut depths with the number of load repetitions for the three sections considered. Each point in the figure represents an average rut depth value from eight measurement stations at 4-ft. intervals under the ALF loading paths. As shown in the figure, during the first 175,000 load repetitions when the ALF load level was at 9,750 lb., the two foamed-asphalt sections (4-3A and 4-3B) apparently performed better than or as well as the stone section of 4-2B. The mean rut depth at 175,000 repetitions was 0.12 in. for the FA/50RAP/50SC section and 0.25 in. for both the FA/100RAP and stone sections. Subsequently, as the load level increased from 9,750 lb. to a higher load magnitude, both foamed-asphalt sections exhibited a significantly higher rate of rutting than the stone section. In the end, the crushed stone section (4-2B) reached a rutting failure limit of an average rut depth of 0.5 in. approximately at ALF loading cycle of 282,000; whereas, the FA/100RAP and FA/50RAP/50SC sections reached the limit at 230,000 and 228,000 repetitions, respectively. When converting the ALF repetitions into the 18,000-lb. ESAL numbers based on the fourth power law, the corresponding ESAL numbers for sections 4-2B, 4-3A, and 4-3B would be 786,000, 411,000, and 356,000, respectively *[26]*.
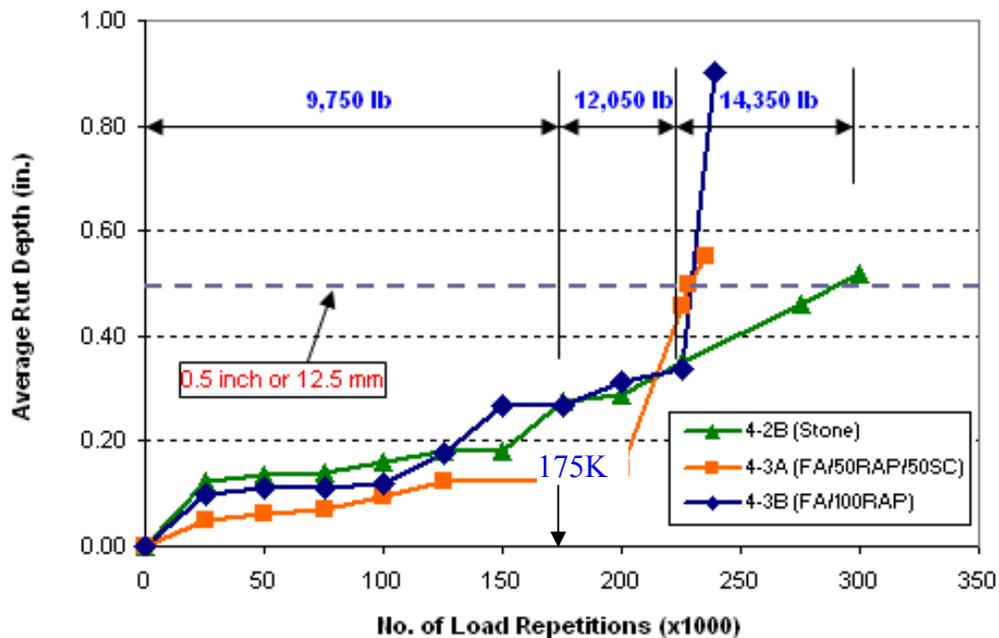
Figure 16
Measured rut depths on test sections

Figure 16 also indicates that the rutting accumulation rate on section 4-3A (containing FA/50RAP/50SC) changed drastically after the load level changed from 9,750 lb. to 12,050 lb. with a sudden increase at the loading number of 200,000. In addition, it showed that the increase of rutting on section 4-3B (containing the FA/100RAP) skyrocketed after the load magnitude increased to 14,350 lb. at 225,000 repetitions. Such a drastic increase in the rate of rutting for the two foamed-asphalt test sections may be well explained by the stress-dependence of pavement base materials using the Shakedown theory *[27], [28], [29], [30]*. The Shakedown theory indicates that most pavement materials are stress-dependent and have a self-specified threshold stress level called the "shakedown load." When limiting the stress level in a pavement material below its threshold stress, it will eventually respond in a resilient (elastic/shakedown) manner as the load repetitions increase. On the other hand, when continuously increasing the stress level and passing its threshold stress, the material will first go to a plastic creep stage and eventually to a stage of incremental collapse. The shakedown analysis indicated that both foamed-asphalt treated RAP base materials seemed to have a lower shakedown threshold stress than the crushed stone base. The increase of the ALF load levels after 175,000 repetitions caused pavement base stresses higher than the shakedown threshold stresses of the two foamed-asphalt treated RAP base materials and eventually resulted in a sudden rutting failure for the two foamed-asphalt test sections. Since both foamed-asphalt base materials had an excellent early performance up to 175,000

32

repetitions when the load level was at 9,750 lb., the shakedown analysis also suggested that, as long as keeping the traffic induced stress level below their corresponding threshold stresses (as shown in the case when the ALF load was at a 9,750 lb. level), both foamed-asphalt base materials may have continuously performed better than the stone base.

NDT Test Results
Pavement surface deflections were measured during the ALF testing by both Dynaflect and FWD methods on each test section at an interval of every 25,000 ALF repetitions.

Dynaflect Results. Figure 17 presents ALF load induced progression of the average SN values for the three test sections evaluated, which were estimated by applying the Dynaflect measured deflections into the Louisiana Pavement Evaluation Chart. A higher SN value indicates a greater structural capacity of a pavement. An initial increase in the SN values during the first 75,000 ALF passes or so may be attributed to the post construction densification of pavement layers and the corresponding material strength gains due to the curing. As expected, the overall SN values generally displayed a slightly decreasing trend (due to pavement deterioration) with the increase of load repetitions.
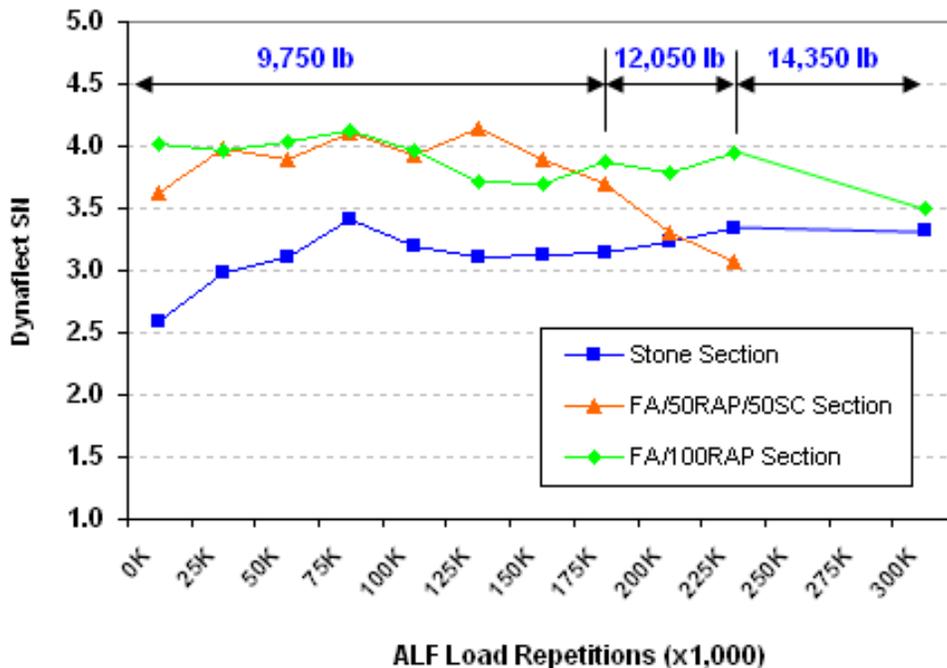
Figure 17
Dynaflect structural number results

As shown in Figure 17, prior to 175,000 loading repetitions, both foamed-asphalt sections had higher SN values than the stone section (4-2B). After 175,000 repetitions, the SN for the FA/50RAP/50SC section (4-3A) began to decrease rapidly and eventually became lower than that of the stone section. Furthermore, due to the increase of ALF load levels, the SN for the FA/100RAP section also showed a sharper decrease after 225,000 repetitions. However, the change in SN values for the stone section was observed not to be sensitive to the changes of ALF load levels, Figure 17.

In general, the progression of SN changes observed for the three test sections matched well with the rutting measurement curves shown in Figure 16. It appeared to indicate that the rapid decreases of SN on the two foamed-asphalt sections directly resulted from the incremental shakedown failure of the foamed-asphalt base layers due to the increase of load magnitudes.

FWD Test Results. Figure 18 presents the average FWD center deflection (D0) test results for the test sections evaluated. The deflection was first normalized to a 9,000-lb. load level and then temperature-corrected to 25°C based on a procedure developed under the Long Term Pavement Performance (LTPP) program *[31]*. The center deflection measured directly under the FWD loading plate is usually considered an indicator of the composite stiffness of a pavement structure. A higher surface deflection indicates a smaller composite stiffness for a pavement structure. It should be noted that FWD deflection results after 225,000 repetitions were not used in the analysis due to significant variations resulting from the excessive surface distresses developed.

As shown in Figure 18, the D0 response curves of all three sections showed an increasing trend with the increase of load repetitions, except for the first 75,000 repetitions on the FA/50RAP/50SC section (4-3A). As mentioned earlier, section 4-3A was not tested at the same period as sections 4-2B and 4-3B. The initial decreasing of D0 on this section could be attributed to the temperature effects as well as the initial pavement layer's further densification and curing. Before 175,000 repetitions, both foamed-asphalt test sections had a smaller D0 than the stone section. Subsequent to 175,000 repetitions, the D0 responses of the FA/50RAP/50SC section started to increase rapidly, indicating a fast deterioration inside the pavement structure of this section. This may be indicative of the failure of the FA/50RAP/50SC base under a higher load level of 12,050 lb., as explained earlier by the Shakedown Theory. On the other hand, both the stone and FA/100RAP sections (4-2B and 4-3B) showed steadily increasing D0 values with load repetitions up to 225,000 repetitions. It should be noted that the shakedown failure was not observed for the FA/100RAP section due

to lack of the FWD data after 225,000 repetitions. Overall, the normalized D0 results were found consistent with the Dynaflect structural number results shown in Figure 17.
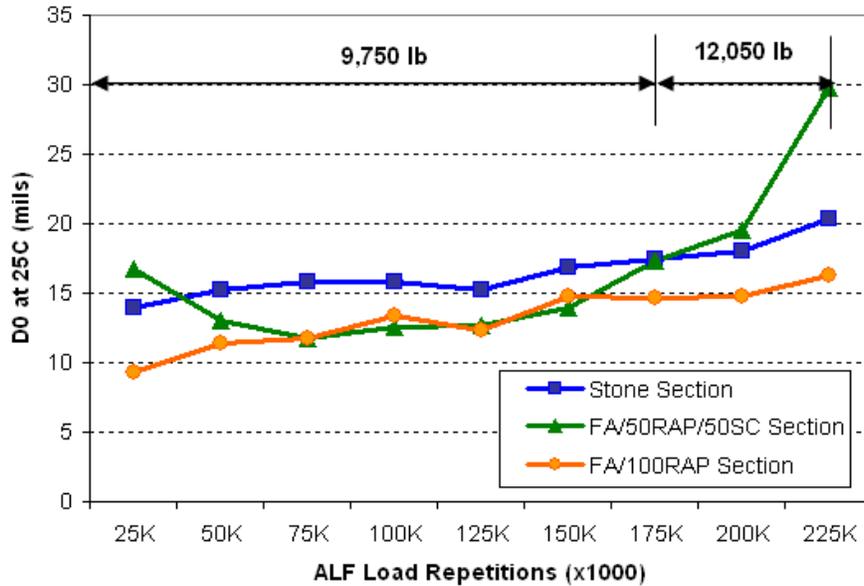
Figure 18
FWD center deflections

Tables 10 through 12 present FWD backcalculation results for sections 4-2B, 4-3A and 4-3B, respectively. It is noted that, in order to obtain a more realistic set of backcalculated layer moduli with acceptable RMS errors, the HMA modulus in all backcaluation trials was assumed to be a constant value of 725 ksi at 25°C. Fixing the input modulus for one or more pavement structure layers is a common practice in the FWD modulus backcalculation, especially when the thickness of a pavement layer is relatively thin, such as the 2-in. HMA layer used in this experiment. The RMS was controlled to be less than 5 percent in the backcalculation. Deflection bowls with high RMS errors were not included in the analysis.

As shown in Tables 10-12, all cement treated layers received high backcalculated moduli, with the highest values found in the FA/100RAP section (4-3B). In addition, during the first 175,000 repetitions, the backcalculated subgrade moduli in the stone section (4-2B) were found to be slightly lower than those in the foamed-asphalt sections (4-3A and 4-3B). This may be explained by the stress-softening property of the silty-clay subgrade soil. High stress in the subgrade layer results in low subgrade modulus.

Table 10
FWD backcalculation moduli for the Stone section (4-2B)

No. of Passes	Cumulative ESALs	Modulus (ksi)			
(K = 1000)	x1000	HMA	Crushed Limestone	Cement Treated Subgrade	Subgrade
0K	0	751.0	32.1	407.9	13.3
25K	34	684.5	48.8	243.9	15.8
50K	69	639.0	42.6	225.9	13.9
75K	103	542.4	40.1	264.1	13.0
100K	138	586.9	44.3	197.5	13.7
125K	172	606.0	45.0	236.3	13.1
150K	207	522.1	44.0	221.7	12.4
175K	241	556.3	48.4	223.7	13.9
200K	321	551.5	39.7	252.6	14.3
225K	402	533.4	32.0	257.9	14.5

Table 11
FWD backcalculation moduli for the FA/50RAP/50SC section (4-3A)

No. of Passes	Cumulative ESALs	Modulus (ksi)			
(K= 1000)	x1000	HMA	FA/50RAP/50SC	Cement Treated Subgrade	Subgrade
0K	0	592.4	125.1	379.5	19.9
50K	69	726.5	55.8	596.3	18.7
75K	103	824.6	62.7	731.5	18.6
125K	172	600.1	53.2	590.6	17.0
175K	241	464.4	51.9	494.9	16.0
200K	321	551.3	27.2	478.0	15.7
225K	402	552.6	17.5	190.1	8.5

Table 12
FWD backcalculation moduli for the FA/100RAP section (4-3B)

No. of Passes	Cumulative ESALs	Modulus (ksi)			
(K= 1000)	x1000	HMA	FA/100RAP	Cement Treated Subgrade	Subgrade
0K	0	858.1	176.5	876.5	20.9
25K	34	658.9	92.6	734.0	17.7
50K	69	551.0	56.0	645.3	19.0
75K	103	579.2	52.8	627.1	18.7
100K	138	421.0	49.7	550.7	18.9
125K	172	590.0	51.6	521.3	19.0
150K	207	429.0	50.0	664.7	17.2
175K	241	489.6	51.5	719.4	16.8
200K	321	498.8	33.9	701.8	18.2
225K	402	530.2	26.8	816.3	17.9

Figure 19 presents the backcalculated moduli for the three base materials considered. As shown in the figure, the moduli for both foamed-asphalt materials decreased rapidly as the load repetitions increased. However, the stone base used in section 4-2B seemed not very sensitive to the load repetitions, whose moduli varied slightly with the increase of load repetitions. It can also be noticed from the figure that both foamed-asphalt bases had a higher backcalculated modulus than the stone base up to 175,000 load repetitions. The rapid decrease in backcalculated modului of those foamed-asphalt materials, although partially due to the temperature effect, may be attributed to the internal stiffness degradation or deterioration due to internal damage, which could be load induced (e.g., shakedown failure) or environmentally induced (e.g., the moisture effect).

Overall, FWD backcalculation results indicated that both foamed-asphalt base materials deteriorated faster than the stone base due to either high stress induced shakedown failure or internal material degradation due to the moisture effect.
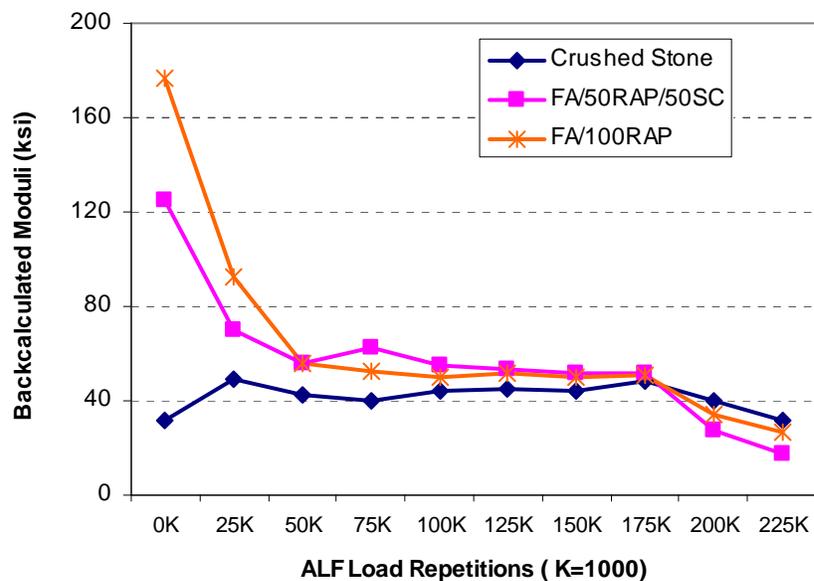
Figure 19
Backcalculated moduli for base materials

Instrument Responses to ALF Wheel Loading

Pressure Cell Measurements. Table 13 presents a statistical summary for the pressure cell measurements at two vertical depths of each test section investigated. Note that the results shown in Table 13 were measured from embedded pressure cells up to 175,000 load repetitions under a 9,750-lb. ALF moving load. Subsequent to 175,000 load repetitions,

pressure cells embedded on the stone section (4-2B) and FA/100RAP section (4-3B) started to malfunction, and thus, the measurements were not included in the analysis. As shown in Table 13, the average vertical stresses developed at the bottom of base layers were 18.6, 10.2, and 9.6 psi for the stone base section (4-2B), the FA/50RAP/50SC section, and the FA/110RAP section, respectively. Meanwhile, the corresponding average stress values on the top of subgrades were 0.7, 0.4, and 0.3 psi, respectively. It can be observed from Table 13 that the coefficients of variation (COV) for the two foamed-asphalt sections (4-3A and 4-3B) were generally higher than those obtained for the stone section (4-2B). This may be because: (1) a foamed-asphalt base layer is more temperature sensitive than the stone, and (2) the moduli of the foamed-asphalt layer were continuously decreasing with load repetitions as shown in Figure 19.

Table 13
Results of the measured vertical compressive stresses

| Section | Statistics | Vertical Stress (psi) | |
		At Bottom of Base	At Top of Subgrade
4-2B	Avg	18.6	0.7
	Std	0.4	0.1
	COV	2.2%	7.7%
4-3A	Avg	10.2	0.4
	Std	1.2	0.1
	COV	12.2%	18.5%
4-3B	Avg	9.6	0.3
	Std	1.5	0.1
	COV	15.7%	9.7%

The pressure cell measurements indicate that the vertical compressive stresses at the bottoms of both base and subbase layers on the stone section (4-2B) were generally larger than those developed on the two foamed-asphalt sections (4-3A and 4-3B). This implies that the crushed stone base of section 4-2B should normally have a lower in-situ stiffness value (or moduli) than both foamed-asphalt base materials under the ALF load of 9,750 lb.

Overall, the recorded vertical stress results generally confirmed the rutting ranking order for the three test sections up to the first 175,000 load repetitions, as shown in Figure 16. Unfortunately, no stress comparison could be made after 175,000 repetitions due to the early failure of pressure cells. The potential shakedown stress levels for the foamed-asphalt base materials could not be determined.

MDD Results. Figure 20 presents MDD measured permanent deformations versus the number of load repetitions for individual pavement layers of the three APT test sections. As shown in Figure 20a, the stone base, cement treated subgrade, and subgrade layers of section 4-2B contributes 85 percent, 5 percent and 10 percent of the total MDD measured permanent deformation, respectively. Figure 20b indicates that almost 95 percent of the final MDD deformation was developed in the FA/50RAP/50SC layer of section 4-3A, and negligible deformation was found for the other two layers on this section. On the other hand, for section 4-3B (Figure 20c), approximately 50 percent of the total measured permanent deformation came from the foamed-asphalt base layer (FA/100RAP), and about 40 percent of the total measurement came from the cement treated subgrade layer, and 10 percent was from the subgrade. As expected, significantly large amounts of permanent deformation were observed on all three base layers investigated in this study.

(a)   (b)

(c)
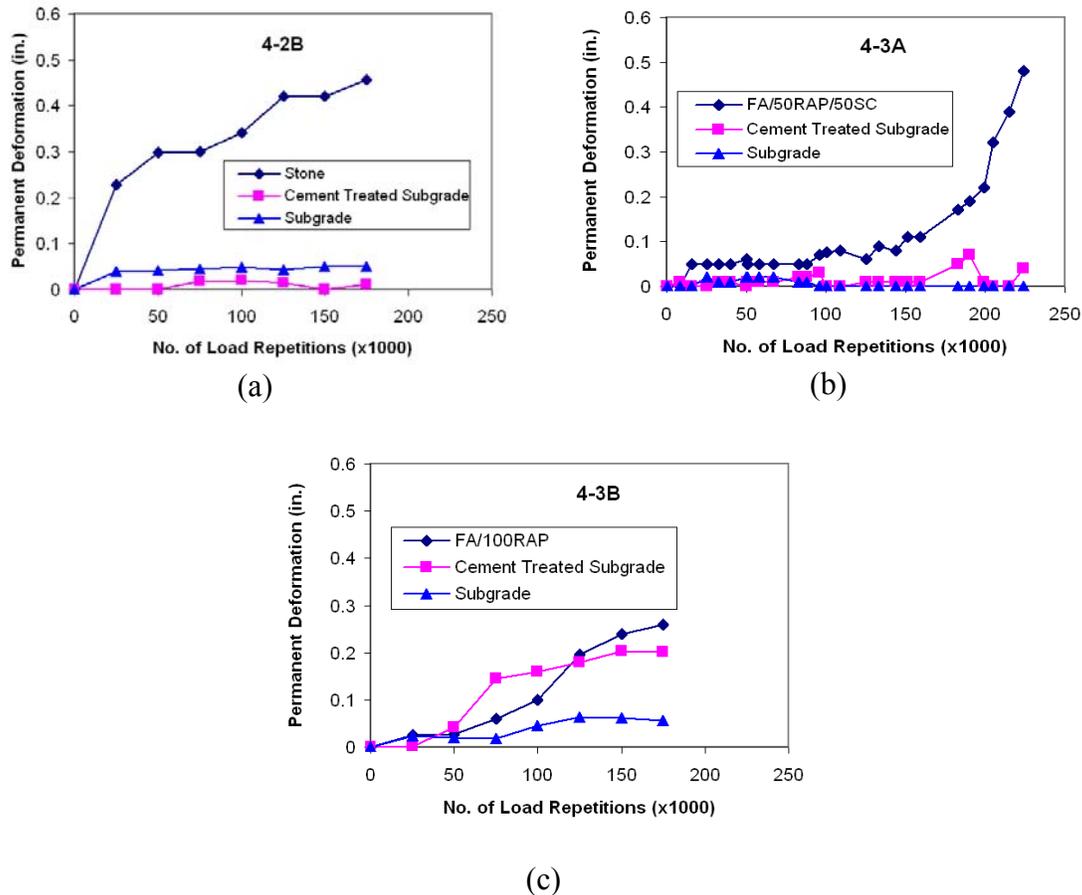
Figure 20
MDD measured permanent deformation at each section

As shown in Figure 20, the load-deformation curves for the three base materials differed significantly from one to the other. The crushed stone base (Figure 20a) was found to develop significantly large permanent deformation during the first 25,000 ALF repetitions, and then the rate of deformation started to slow down and showed a decreasing trend until the end of the MDD measurements of 175,000 ALF passes. On the other hand, both foamed-asphalt base layers initially developed very small amounts of permanent deformation. The rate of deformation rate started to take off at 175,000 ALF load repetitions on section 4-3A and at 100,000 repetitions on section 4-3B.

As described in the preceding section, the difference in the permanent deformation development process among the three base materials investigated can be well explained by the Shakedown Theory *[27]*. By plotting the vertical permanent strain rate (permanent strain per load cycle) versus the vertical permanent strain, the behavior of a pavement material can be divided into three different categories *[30]*:

- Range A–plastic shakedown range: The response is plastic only for a finite number of load applications and becomes purely resilient after completion of the post-compaction. The permanent strain rate quickly decreases to a very small level.
- Range B–intermediate response (plastic creep): The level of permanent strain rate decreases to a low and nearly constant level during the first several loading cycles.
- Range C–incremental collapse: The permanent strain rate decreases very slowly or not at all, and there is no cessation of permanent strain accumulation.

While Range A is generally expected for a well-designed, good-performing pavement layer and Range B materials can be acceptable under certain pavement conditions, materials with a Range C performance should always be avoided. Based on the MDD permanent deformation results, the three base materials used in the APT test sections did experience different shakedown responses. It was found that the crushed stone had a Range B response, while the FA/50RAP/50SC base had a Range C response. It should be pointed out that, due to limited MDD data, the characterization for the FA/100RAP material could not be performed. Further, if limiting the ALF load to a level of 9,750 lb., the FA/50RAP/50SC material could not be performed in the Range B category as the stone base investigated. This information provided some field evidence in favor of using the Shakedown Theory in describing pavement material responses *[30]*.

Rutting Prediction using VESYS

As mentioned in the methodology section, the rutting performance of test sections was simulated using the VESYS 5W computer program. Table 8 presents the determined

permanent deformation parameters (μ and α) for the three base materials from the laboratory permanent deformation test. VESYS default input values were used for other layers including the HMA, cement treated subgrade, and subgrade, since this simulation was focused on the base layers. In addition, the FWD backcalculated moduli, as shown in Tables 10-12, were used in the analysis to represent the average in-situ material conditions.

Figures 21 (a)-(d) present the VESYS predicted rut depth results as compared to the measured rut depths up to 225,000 load repetitions. As shown in Figure 21(a), the final predicted rut depth for section 4-2B was 0.51 in., for section 4-3A it was 0.88 in. and for section 4-3B it was 1.30 in. As shown in Figures 21(b)-(d), the predicted rut depths were about 45 percent higher than the field results for section 4-2B, 92 percent higher for section 4-3A, and 285 percent higher for section 4-3B.

(a)

(b)

(c)

(d)
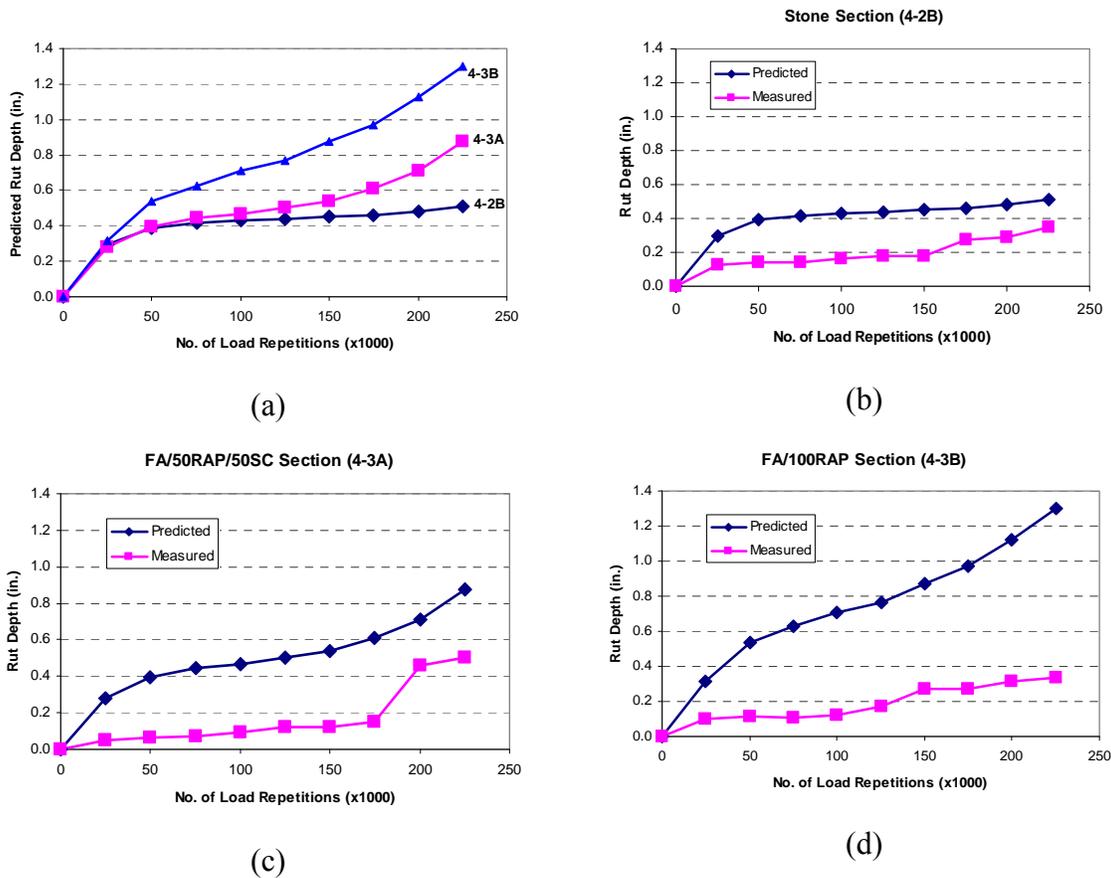
Figure 21
Comparison of VESYS predicted rut depth for all three sections

VESYS also predicts individual layer rutting contribution in terms of percent contribution to the total surface rut depth, as shown in Figure 22. All base layers showed significantly high

rutting contributions to the total surface rut depths. The stone base in section 4-2B contributes 34.9 percent of total rutting, the FA/50RAP/50SC contributes 60 percent, and the FA/100RAP contributes 74.6 percent. If not considering the HMA layer contribution, the predicted base contribution becomes about 51 percent for the stone layer on section 4-2B and 76 percent for the FA/50RAP/50SC on section 4-3A. Since the VESYS prediction represents the average performance of a test section, the predicted rutting contribution on sections 4-2B and 4-3A are considered acceptable even though they are different from the MDD measured results as shown in Figure 20. However, those predicted rutting contributions for section 4-3B are completely different from the MDD measurements on this section. Because section 4-3B failed due to excessive surface cracking and the required input parameters for cracking prediction in VESYS was not available in this study, the rutting prediction results for section 4-3B were considered not valid. However, it did reflect the weakness of the FA/100RAP layer used in this section.
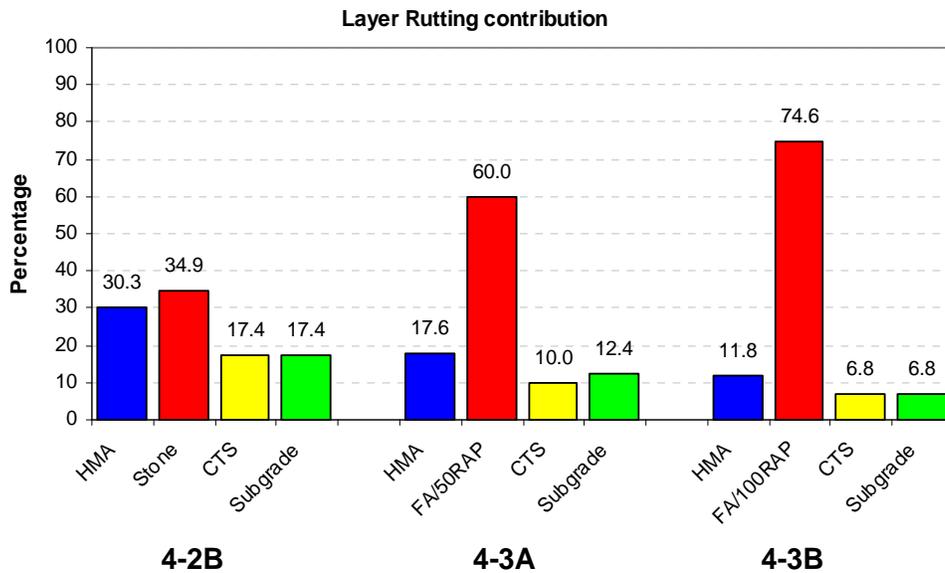
Figure 22
VESYS predicted layer rutting contribution

In conclusion, the rutting prediction using VESYS may be considered partially successful in this study. The prediction results demonstrated that VESYS could capture the overall performance of a pavement structure under the ALF loading. In addition, the rutting development trends and layer contributions were considered similar to the field observed results. Although the prediction results over-estimated the rut depths by a significantly large margin, the VESYS rutting simulation analysis generally confirmed the APT performance of the three base materials investigated in which both foamed-asphalt treated RAP bases did not

perform as well as the stone base under the ALF experiment condition. Considering those default input values used in the prediction, more accurate input parameters are recommended to use in future performance prediction using VESYS.

Failure Analysis of Foamed-Asphalt Base Materials

The aforementioned Shakedown Theory indicates that both foamed-asphalt treated RAP base materials had a lower shakedown stress than the crushed stone base, which resulted in a rapid increase in the rate of rutting under a higher ALF load level. However, it is not known why the asphalt bonded materials could possibly have a lower shakedown stress, which means a lower load carrying capacity than the stone material. A failure investigation was performed on the two foamed-asphalt test sections and the following observations were made.

Laboratory wheel tracking rut tests showed that both foamed-asphalt materials exhibited low water resistance when tested in a submerged condition and the FA/50RAP/50SC material exhibited even greater moisture susceptibility than the FA/100RAP material.

The foamed-asphalt mix design data (Table 2) indicate that both foamed-asphalt base materials had high design air voids and relatively low indirect direct strength. The design air voids for FA/50RAP/50SC material was 20.3 percent, even higher than 15.3 percent for FA/100RAP material.

Post-mortem trench results indicated that, as shown in Figure 23(a), the transverse rutting profile of section 4-2B (the stone base section) primarily resulted from further densification of the HMA and crushed stone materials under the load. However, the rutted profiles showed on the foamed-asphalt sections [Figures 24(b) and 24(c)] included not only densification (depression below the original surface) but also heave deformation (permanent deformation above the original surface). The heave deformation was generally rooted from the base layers of sections 4-3A and 4-3B. Such an observation indicates that both foamed-asphalt treated base materials had a shear failure due to insufficient shear strengths to resisting the ALF load induced shear stress, especially under the increased ALF load levels. As compared to the crushed stone base, insufficient shear strength of foamed-asphalt treated materials may result from insufficient bonds between foamed-asphalt and treated materials and some lubrication effects of asphalt binder under higher temperatures and wet environments.
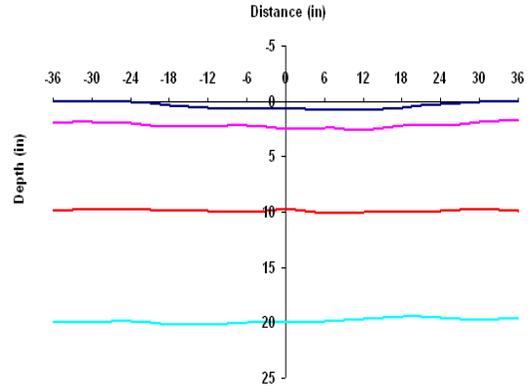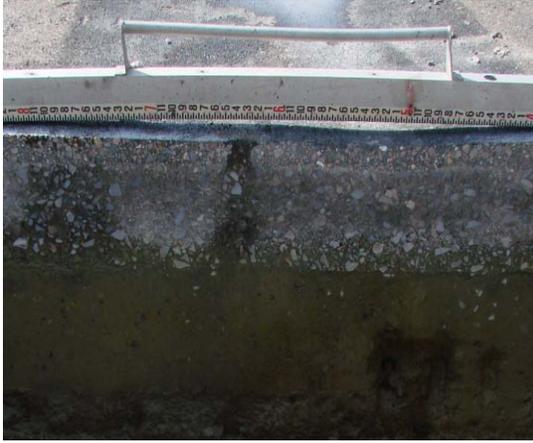
(a) Section 4-2B
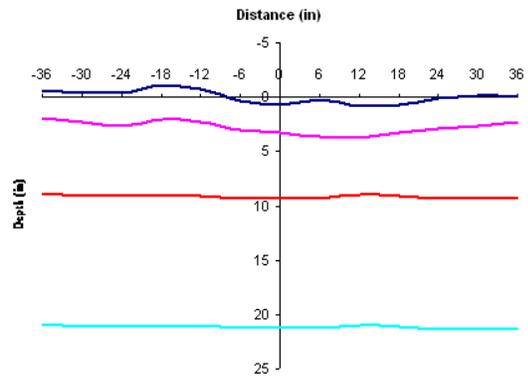
(b) Section 4-3A
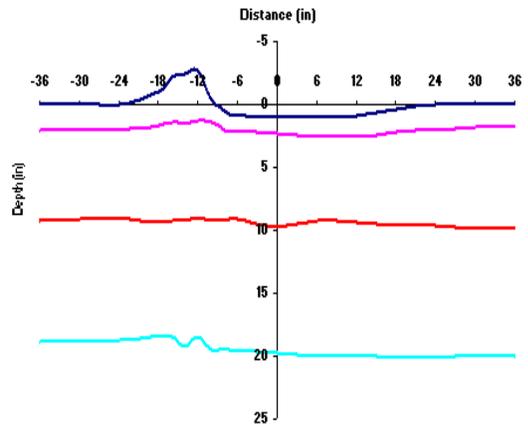
(c) Section 4-3B

Figure 23
Post-mortem trench results

The trench profiles also revealed that, while negligible permanent deformations were found below the base layers of both sections 4-2B and 4-3A, the cement treated subgrade and subgrade layers on the FA/100RAP section (4-3B) did show some permanent deformation development. This observation is consistent with the MDD results showed in Figure 20.

It was noticed several months after construction that small droplets of asphalt binder material had seeped up through the surface of section 4-3B (with FA/100RAP base). As shown in Figure 24, those initially spotted asphalt droplets became much more noticeable during the APT testing and eventually caused significant surface distresses on section 4-3B (Figure 15). A droplet binder sample was obtained from section 4-3B for a performance grading test analysis using the Dynamic Shear Rheometer (DSR). Test results conducted on the original droplet material indicated a high temperature grading of PG 82. In addition, the construction record showed that a MC-250 cutback asphalt was used as a prime coat on top of both foamed-asphalt layers with a measured 0.25 gallons per square yard. It is believed that the droplet binder material was a combination of the foamed-asphalt, RAP, and prime coat materials of the test section that bled through the surface.

Figure 24
Asphalt droplets on section 4-3B

Based on above laboratory and field observations, the following hypothesis could be made to explain why the two foamed-asphalt treated RAP materials failed prematurely in this APT study:

- The early failure on the FA/50RAP/50SC section (4-3A) could be attributed to both water susceptibility and a weak aggregate skeleton used in the FA/50RAP/50SC base mixture. First, the free moistures could have entered into the FA/50RAP/50SC base layer through the surface cracks developed around the MDD location. (It was noticed during the APT testing that the surrounding pavement area around the MDD cap in this section developed some surface cracks after 100,000 repetitions.) Free surface water could have gone into the base layer through those surface cracks. Second, this mixture consisted of 50 percent RAP, 50 percent recycled soil cement, and a design air void of 20.3 percent. The high percentage of recycled soil cement material had potentially produced a weak structural skeleton for the FA/50RAP/50SC mixture (i.e., too much soil particles). Therefore, only 2.8 percent foamed-asphalt content may be not able to bond the weak aggregate skeleton effectively. Consequently, when enduring high load-induced stresses under a moisture rich pavement condition, this material suddenly lost its strength and started to develop a shear failure.

- The early failure on section 4-3B could be attributed to both water susceptibility and over-asphalting in the FA/100RAP mixture. In addition, the FA/100RAP mixture contained 97.5 percent RAP and 2.5 percent foamed-asphalt. The aged RAP binders plus the foamed-asphalt cement could have prevented the foamed-asphalt mixture from absorbing the additional prime coat materials. Consequently, under the daily temperature change (especially during a summer), the free asphalt materials started to seep up through the top HMA layer. Such "seep-up" action not only caused a cosmetic problem, but it also created many tiny crack paths inside the HMA mixture. Therefore, free surface moistures could have entered into the FA/100RAP base layer through those cracks, which gradually weaken the strength of the base material, causing a premature shear failure.

In summary, the following lessons may be learned: (1) more research on how to design a foamed-asphalt treated RAP and other recycled materials is still needed; (2) the use of a prime coat layer on top of a foamed-asphalt treated RAP layer should be cautioned; (3) the foamed-asphalt treated RAP materials should not be used in any moisture-rich environments; (4) due to the excellent early performance under the 9,750 lb. ALF load, the foamed-asphalt mixtures of this study may be suitable to use as a base course material for the low volume roads in Louisiana, where the percentage of heavy truck traffic is relatively low and the environment is relatively dry (or has a good drainage system).

Economic Analysis

The following table lists a breakdown of the unit costs for major items in the construction of a foamed-asphalt treated RAP base (based on the dollar value of 2003):

RAP	$ 1.38 /yd^2 (unit price of $4 /ton)
2.5% Asphalt Cement (PG 58-22)	$ 2.50 /yd^2
1.0% Cement	$ 0.51 /yd^2
Average Placement Cost	$ 1.00 /yd^2
Total Construction Cost	$ 5.39 /yd^2

It should be noted here that the unit costs for RAP materials depends on the transportation cost and is project specific. According to the contractor of this project and past experience on the crushed stone base construction, the average construction cost for the crushed stone base is approximately $7.50 dollars per square yard. The above analysis indicates that, when RAP materials are largely available and have a reasonable transportation cost, using a foamed-asphalt treated RAP base in pavement construction has a potential to save construction costs compared to using a crushed stone base.

CONCLUSIONS

An APT experiment was conducted using the ALF (Accelerated Loading Facility). The APT experiment included three test sections: the first one contained a foamed-asphalt treated 100 percent RAP base course (called FA/100RAP), the second used a foamed-asphalt treated 50 percent RAP and 50 percent recycled soil cement base course (called FA/50RAP/50SC), and the third had a crushed stone base. Despite using different base materials the three APT sections shared other pavement layers and had a common pavement structure. Each test section was instrumented with one multi-depth deflectometer and two pressure cells. Surface distress surveys and non-destructive deflection tests were performed at every 25,000 ALF load passes. In addition, a series of laboratory engineering performance-based tests were performed to characterize the performance of utilized materials in the APT experiment. The following observations and conclusions may be made from this study:

- Laboratory test results indicated that the HMA mixture used in the APT test sections had a rutting resistance similar to those obtained for well-performing Superpave mixtures in the state of Louisiana. In addition, the SCB, ITS, $ITSM_R$, and E* test results showed that this mixture had good fatigue endurance at intermediate and low temperatures.
- Hamburg wheel loading test results confirmed that both foamed-asphalt treated RAP mixtures had high water susceptibilities when tested in a submerged condition.
- The overall APT performance indicated that the two foamed-asphalt base materials did not perform as well as the crushed stone base evaluated. A shakedown rutting failure (or incremental collapse) was found on both foamed-asphalt test sections. The shakedown analysis indicated that both foamed-asphalt treated RAP base materials seemed to have a lower shakedown threshold stress than the crushed stone base evaluated.
- Field measurement results showed that both foamed-asphalt test sections had a better performance with a greater structural capacity and rutting resistance than the crushed stone section during the first 175,000 ALF load repetitions when the applied ALF load was at 9,750 lb. The backcalculated in-situ moduli for the two foamed-asphalt base courses during this loading period were found to be higher than that of the crushed stone base. It was the increase of the ALF load levels that caused pavement base stresses higher than the shakedown threshold stresses of the foamed-asphalt bases and eventually resulted in a shakedown failure for the two foamed-asphalt test sections.

- Forensic investigation revealed that the early failure on the FA/50RAP/50SC section could be attributed to both water susceptibility and weak aggregate skeleton design of the foamed-asphalt mixture used; whereas, the premature failure on the FA/100RAP section was due to the combination of poor water resistance of the foamed-asphalt mixture as well as an over-asphalting problem found in this section.
- Cost analysis showed that, when RAP materials are largely available and have a reasonable transportation cost, using a foamed-asphalt treated RAP base in pavement construction has a potential to save construction costs as a comparison of using a crushed stone base.

RECOMMENDATIONS

Due to the potential cost benefit and excellent performance under an ALF load of 9,750 lb., the two foamed-asphalt mixtures evaluated in this study could be used as an alternative to other base course materials on low volume roads in Louisiana, where the percentage of heavy truck traffic is very low and the environment is relatively dry (or has a good drainage system).

ACRONYMS, ABBREVIATIONS, AND SYMBOLS

AASHTO	American Association of Highway and Transportation Officials
AC	Asphalt Concrete
ALF	Accelerated Load Facility
APA	Asphalt Pavement Analyzer
APT	Accelerated Pavement Testing
COV	Coefficient Of Variance
DOT	Department of Transportation
Dynaflect	Dynamic Deflection Determination System
D1	Deflection Measured at Center of FWD Plate
ESAL	Equivalent Single Axle Load
FA	Foamed-asphalt
FSCH	Frequency Sweep at Constant Height
FWD	Falling Weight Deflectometer
HMA	Hot Mix Asphalt
ITC	Indirect Tensile Creep
Jc	Critical Strain Energy Release Rate
LADOTD	Louisiana Department of Transportation and Development
LTRC	Louisiana Transportation Research Center
LTPP	Long Term Pavement Performance
LWT	Loaded Wheel Tester
MDD	Multi Depth Deflectometer
M_r	Resilient Modulus of Subgrade
MTS	Material Testing System
NDT	Non-Destructive Testing
PI	Plastic Index
PMLC	Plant-Mixed Laboratory-Compacted
PRF	Pavement Research Facility
RAP	Reclaimed Asphalt Pavement
RLT	Repeated Load Tri-axial
RMS	Root Mean Square
SC	Soil Cement
SCB	Semi-Circular Bending
SN	Structural Number
TI	Toughness Index

REFERENCES

1. Csanyi, Y.H. "Foamed-asphalt in Bituminous paving Mixtures." *Bull. 160. HRB*, National Research Council, Washington, D.C., 1957, pp. 108-122.

2. Roberts, F.L., Engelbrecht, J.C., and Kennedy, T.W. "Evaluation of Recycled Mixtures Using Foamed Asphalt." *Transportation Research Record No. 968*, TRB, National Research Council, Washington D.C., 1984, pp. 78-85.

3. Nataatmadja, A. "Some Characteristics of Foamed Bitumen Mixes." *Transportation Research Record, No. 1767*, TRB, National Research Council, Washington D.C., 2001, pp. 120-125.

4. Bowering, R.M. and Martin, C.L. "Foamed Bitumen Production and Application of Mixtures – Evaluation and Performance of Pavements." Association of Asphalt Paving Technologists, Vol. 45, 1976, pp. 453-477.

5. Lee, D.Y. "Treating Marginal Aggregates and Soils with Foamed Asphalt." Proceedings of Association of Asphalt Paving Technologists, Vol. 50, 1981, pp. 211-250.

6. Little, D.H., Bulton, J.W. and Epps, J.A. "Structural Properties of Laboratory Mixtures of Foamed Asphalt and Marginal Aggregates." *Transportation Research Record, No. 911,* TRB, National Research Council, Washington D.C., 1983, pp. 103-113.

7. Sakr, H.A. and Manke, P.G. "Innovations in Oklahoma Foamix Design Procedures." *Transportation Research Record No. 1034*, TRB, National Research Council, Washington D.C., 1985, pp. 26-34.

8. Bissada, A. "Structural Response of Foamed-asphalt Sand Mixtures in Hot Environment." *Transportation Research Record No. 1115*, TRB, National Research Council, Washington D.C., 1987, pp. 134-149.

9. Brenne, M., Tia, M., Altschaeffl, A. and Wood, L.E. Laboratory Investigation on the use of Foamed-asphalt for Recycled Bituminous Pavements. *Transportation Research Record, No. 911*, TRB, National Research Council, Washington D.C., 1983, pp. 80-87.

10. Smith M. "What is Foamed Asphalt?" Southern Research Center, Federal Highway Administration, http://www.fhwa.dot.gov/resourcecenters/southern/innovmat.htm.

11. Wirtgen Cold Recycling Manual, Wirtgen GmbH, Hohner Straße 2, D-53578 Windhagen, Nov., 1998.

12. Mohammad, L., Farsakh, M., Wu, Z., and Abadie, C. "Louisiana Experience with Foamed Recycled Asphalt Pavement Base Materials." *Journal of Transportation Research Record No. 1832*, 2003, pp17-24.

13. Marquis, B. Using Foamed Asphalt on a Stabilizing Agent in Full Depth Reclamation of Route 8 in Belgrade, Technical Report 02-2, Maine Department of Transportation, 2009.

14. Chen, D., Bilyeu, J., Scullion, T., Nazarian, S. and Chiu, C. "Failure Investigation of a Foamed Asphalt Highway Project." *ASCE Journal of Infrastructure Systems*, Vol. 12, No. 1, March 2006, pp. 33-40.

15. Louisiana Standard Specifications for Roads and Bridges. State of Louisiana, Department of Transportation and Development, Baton Rouge, 2006 Edition.

16. Gautreu, G., Zhang, Z., Wu, Z. Accelerated Loading Evaluation of Subbase Layers in Pavement Performance, Report No. FHWA/LA.09/468, Louisiana Transportation Research Center, 2010.

17. Wu, Z., Zhang, Z., and King, W. Accelerated Loading Evaluation of Stabilized BCS Layers in Pavement Performance, Draft Final Report, Louisiana Transportation Research Center, 2010.

18. Mohammad, L.N., Wu, Z. and Aglan, M. "Characterization of Fracture and Fatigue Resistance of Recycled Polymer-Modified Asphalt Pavements," *Proceedings of the RILEM: 5th International Conference on Cracking in Pavements Mitigation, Risk Assessment and Prevention*, Edited by Petit, C., Al-Qadui, I., and Millien, A., Limoges, France, May 5–8, 2004, pp. 375–382.

19. AASHTO T 307. "Determining the Resilient Modulus of Soils and Aggregate Materials, American Association of State Highway and Transportation Officials, T 399-07. ME.

20. Guide for Mechanistic-Empirical Design of New and Rehabilitated Pavement Structures, Part 2, Design Inputs, National Cooperative Highway Research Program (NCHRP), NCHRP 1-37A, Final Report, March 2004.

21. Kinchen, R.W. and W.H. Temple. *Asphalt Concrete Overlays of Rigid and Flexible Pavements*. Report No. FHWA/LA-80/147, Louisiana Department of Transportation and Development, 1980.

22. Pierce, L. M., and Mahoney, J. P. "Asphalt Concrete Overlay design Case Studies." *Transportation Research Record 1543*, Transportation Research Board, Washington, D.C., 1996, pp.3-9

23. Kenis, W., Sherwood J. A., and McMahon, T.F. "Verification and Application of The VESYS Structural Subsystem."*The Fifth International Conference on the Structural Design of Asphalt Pavements*. The Delft University of Technology, August 1982.

24. Zhou, F. and Scullion, T. Input Parameters of Enhanced VESYS5, FHWA/TX-05/9-1502-014, Texas Transportation Institute, 2004.

25. Obulareddy, S. "Characterization of Louisiana Asphalt Mixtures for 2002 Mechanistic-Empirical Design Procedure." Master's Thesis, Louisiana State University and Agricultural and Mechanical College, Baton Rouge, Louisiana, USA, 2006

26. Huang, Y. *Pavement Analysis and Design*, Prentice Hall, 1993.

27. Sharp, R. and J. Booker. "Shakedown of Pavements under Moving Surface Loads." *Journal of Transportation Engineering*, ASCE, 110(1), 1984, pp.1-14.

28. Werkmeister, S. *Permanent Deformation Behavior of Unbound Granular Materials*. Ph.D. dissertation, University of Technology, Dresden, Germany, 2003.

29. Arnold, G. K. *Rutting of Granular Pavements*, Ph.D. dissertation, School of Civil Engineering, The University of Nottingham, The United Kingdom, 2004.

30. Tao, M., Mohammad, L., Nazzal, M. Zhang, Z. and Wu, Z. "Application of Shakedown Theory in Characterizing Traditional and Recycled Pavement Base Materials." *Journal of Transportation Engineering*, ASCE, 136 (3), March 2010.

31. Lukanen, E.O., Stubstad, R. and Briggs, R. *Temperature Predictions and Adjustment Factors for Asphalt Pavement*. Publication No. FHWA-RD-98-085, June 2000.

32. Mohammad, L. N., and Paul, H. R. "Evaluation of the Indirect Tensile Test for Determining the Structural Properties of Asphalt Mix." National Academy of Science, *Transportation Research Record No.1417*, 1993, pp. 58-63.

33. American Association of State Highways and Transportation Officials. *Determining the Dynamic Modulus of Hot-Mix Asphalt Concrete Mixtures*. AASHTO Designation TP-62-03.

34. Bonaquist, R.F., Christensen, D.W., and Stump, III., W. *Simple Performance Tester for Superpave Mix Design: First-Article Development and Evaluation*. National Cooperative Highway Research Program (NCHRP) Report 513, Transportation Research Board, National Research Council, Washington, D.C., 2003

35. Mohammad, L. N., Saadeh, S., Zhang, C, Raghavendra, A., *Physical and Mechanistic Properties of HMA mixtures: Field vs. Laboratory*, Report No. FHWA/LA.06/412, Louisiana Transportation Research Center, Baton Rouge, LA, 2006.

36. Mohammad, L.N., Wu, Z. and Raghavendra, A. *Performance Evaluation of Louisiana Superpave Mixtures*. Report No. FHWA/LA.06/410, Louisiana Transportation Research Center, Baton Rouge, LA, 2003.

37. Mohammad, L.N., Kabir, Md, Cooper, S., and Raghavendra, A. "Evaluation of Superpave Mixtures Containing Hydrated Lime" Report No. FHWA/LA/432, Louisiana Transportation Research Center, Baton Rouge, LA, 2008.

APPENDIX

Laboratory Characterization of HMA Mixture

During the construction of APT test sections, sufficient plant-mixed loose HMA mix as well as field cores were collected and used to prepare laboratory testing specimens for different mechanical tests. Laboratory specimens, fabricated through a reheating process from the plant-mixed mixtures, are hereafter referred to as PMLC (plant-mixed lab- compacted) samples. The tests conducted on PMLC samples included: indirect tensile strength (ITS), indirect tensile creep (ITC), indirect tensile resilient modulus (ITM$_r$), semi-circular bending (SCB), dynamic modulus (E*), flow time (FT), flow number (FN), frequency sweep at constant height (FSCH), and loaded wheel tracking (LWT) tests. Only ITS, ITC, ITM$_r$, FT, and FN were conducted on field core samples. The cylindrical samples for ITS, ITC, and ITM$_r$ tests were 4 in. in diameter and about 2.5 in. in height. Samples that are 5.91 in. in diameter by 2.0 in. in height were prepared for FSCH tests. The dynamic modulus, flow number, and flow time tests were conducted on samples that are 4 in. in diameter and 5.91 in. in height. Finally, the SCB test samples were prepared by slicing the 5.91 in. by 2.25 in. high cylindrical samples along their central axes into two samples. A vertical notch was then introduced along the symmetrical axis of each SCB sample in order to examine the true fracture properties of asphalt mixtures with regard to the crack propagation. In addition, slab samples that are 3.2 in. thick, 10.2 in. wide, and 12.6 in. long were prepared for the LWT tests. Those samples were compacted using a kneading compactor. All specimens of PMLC were compacted to 7 ± 0.5 percent air voids.

The detailed description of each test performed is presented below.

HMA Testing Protocols

Load Wheel Tracking Test. Two types of LWT testing devices were used in this study, namely the Hamburg wheel tracking device and asphalt pavement analyzer. The Hamburg test is considered a torture test that produces damage by rolling a 158-lb. steel wheel across the surface of a slab that is submerged in 122°F (50°C) water for 20,000 passes at 56 passes a minute. A maximum allowable rut depth of 0.24 in. at 20,000 passes is used in LADOTD specifications *[15]*. Figure 25 shows the Hamburg wheel tracker used in the study. The second LWT test device used in this study was the asphalt pavement analyzer (APA). This device simulates actual road conditions by rolling a metal wheel over a rubber hose pressurized at 100 psi. The hose stays in contact with the sample's surface while the wheel rolls back and forth along the length of the hose for 8,000 cycles. This test is conducted at 147°F (64°C).
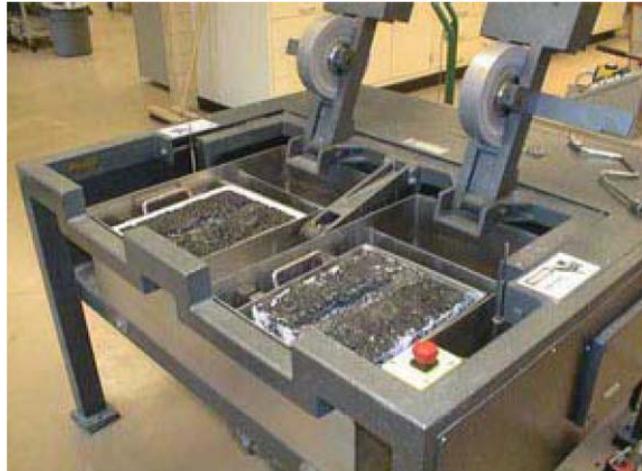
Figure 25
Hamburg LWT device

     Semi-Circular Bend Test. The fracture resistance of the HMA mixture was investigated using the J-integral approach. This procedure is based on a fracture mechanics concept –the critical strain energy release rate, also called the critical value of J-integral, or J_c. In this study, the fracture resistance of the designed mixtures was characterized using this test based on notched semi-circular specimens *[18]*. The method accounts for the flaws as represented by a notch, which in turn, reveals the material's resistance to crack propagation or what is called fracture resistance. During the test, the specimen was loaded monotonically to failure at a constant cross-head deformation rate of 0.02 in./min in a three-point bend load configuration, as shown in Figure 26. The load and deformation were continuously recorded, and the critical value of J-integral (J_c) was then determined as follows:

$$J_c = -\left(\frac{1}{b}\right)\frac{dU}{da}$$
(7)

where,
b = specimen thickness,
a = notch depth, and
U= total strain energy to failure, i.e., the area up to fracture under the load-deflection plot.

To determine the critical value of J-integral, semi-circular specimens with at least two different notch depths need to be tested for each mixture. In this study, three notch depths of 1 in., 1.25 in., and 1.5 in. were selected based on an a/rd ratio (the notch depth to the radius

of the specimen) of between 0.5 and 0.75. For each notch depth, three duplicates were tested. The test temperature used in this study was 77°F.
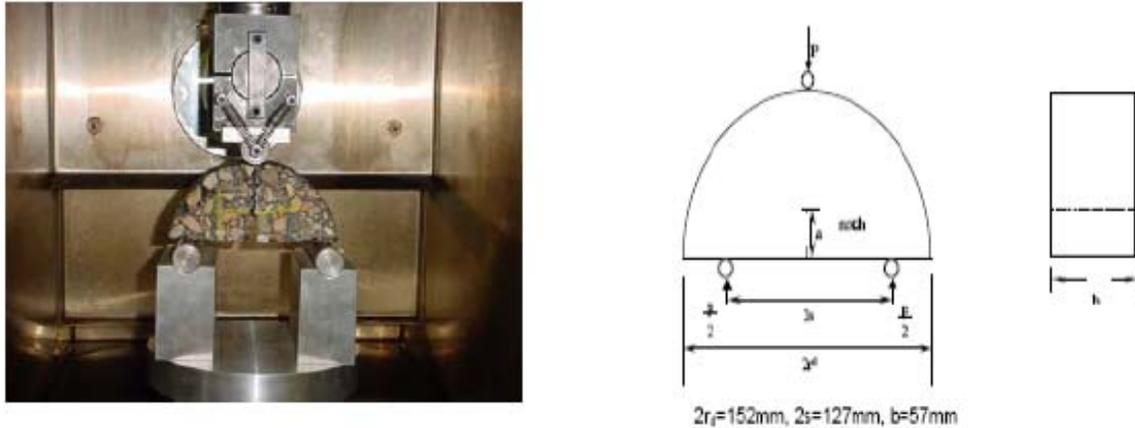
Figure 26
Semi-circular test setup

Indirect Tensile Strength Test. The indirect tensile stress and strain test was used to determine the tensile strength and strain of the HMA mixture. This test was conducted at 77°F in accordance with AASHTO T245 (Figure 27). The test specimen was loaded to failure at a 2 in./min. deformation rate. The load and deformations were continuously recorded. The indirect tensile strength and strain was then computed as follows:

$$ITS = \frac{2P}{2\pi DT} \tag{8}$$

$$\varepsilon_t = 0.52 H_t \tag{9}$$

where,
P = the peak load, lb;
D = the specimen diameter, in;
T = the specimen thickness, in; and
H_t = horizontal deformation at peak load, in.

Toughness Index, a parameter that describes the toughening characteristics of the mixture in the post-peak stress region was also computed from thess test results. A dimensionless indirect tensile toughness index (TI), is defined as follows:

$$TI = \frac{(A_\varepsilon - A_p)}{(\varepsilon - \varepsilon_p)} \tag{10}$$

where,

TI = Toughness Index,

A_ε = Area under the normalized stress-strain curve up to strain ε,

A_p = Area under the normalized stress-strain curve up to strain ε_p,

E = Strain (here, 3 percent) at the point of interest, and

ε_p = Strain corresponding to the peak stress.

Figure 27
Indirect tensile strength test setup

Indirect Tensile Resilient Modulus Test. This test is conducted by applying repeated haversine loads along a vertical diametric plane of the sample. The resulting vertical and horizontal deformations are measured, and the resilient modulus is then computed. The samples in this study were tested at three different temperatures: 41, 77, and 104°F.

Indirect Tensile Creep Test. In this test, a compressive load of 250 lb. was applied on the sample using the stress controlled mode of the MTS test system for 60 minutes or until sample failure *[32]*. The testing temperature of 104°F was used in this study. The deformations acquired during this loading time were used to compute the creep modulus as follows:

$$S(T) = \frac{3.59P}{t \cdot \delta V(T)} \tag{11}$$

where,

S(T) = creep modulus at time *T*, psi;
P = applied vertical load, lb.;

t   = sample thickness, in.; and

δV(T) = vertical deformation at time *T*, in.

The creep modulus versus time is graphed on a log-log scale and used in the analysis.

Dynamic Modulus Test (E*). The dynamic modulus test was performed on unconfined specimens in accordance with AASHTO Standard TP62-03 and an NCHRP Report *[33], [34]*. Figure 28 shows the test set-up. The stress-to-strain relationship under a continuous sinusoidal loading for linear viscoelastic materials is defined by a complex number called the "complex modulus" (E*). The absolute value of the complex modulus, |E*|, is defined as the dynamic modulus. Mathematically, the dynamic modulus is defined as the maximum (i.e., peak) dynamic stress (σ_o) divided by the peak recoverable strain (ε_0):

$$\left|E*\right| = \frac{\sigma_o}{\varepsilon_o}$$

(12)

A sinusoidal compressive stress was applied to test samples at 39.2, 77, 100, and 129.2°F (-10, 4, 25, 38, and 54°C) with loading frequencies of 0.1, 0.5, 1.0, 5, 10, 25 Hz at each temperature to achieve a targeted vertical strain level of 75-100 micro strain. An increasing order of temperature (starting with the lowest temperature and proceeding to the highest one) was maintained throughout the test. Testing at a particular temperature began with the highest frequency of loading and proceeded to the lowest one. Triplicate samples were tested in this study.
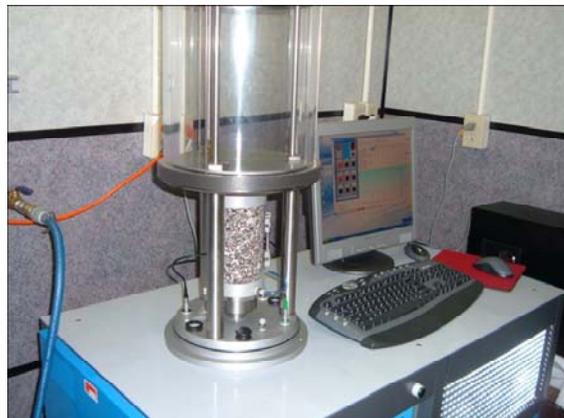
Figure 28
Dynamic modulus test apparatus

Frequency Sweep at Constant Height Test. As described in test procedure E of the AASHTO TP7, the frequency sweep at constant height test is a controlled strain test that applies a shear stress to a cylindrical test specimen to produce a shear strain with a peak amplitude of 1.97E-05 in./min. Sinusoidal shear loading is applied at a sequence of 10 frequencies (10, 5, 2, 1, 0.5, 0.2, 0.1, 0.05, 0.02, and 0.01 Hz) to produce a sinusoidal shear strain. The material property obtained from this test was the dynamic shear modulus and phase angle. The dynamic shear modulus is defined as the ratio of the peak stress amplitude to the peak strain amplitude. Phase angle (δ) is calculated from the time lag between the applied shear stress and the corresponding shear strain. The phase angle for asphalt mixtures will always be between 0 degrees (totally elastic response) and 90 degrees (totally viscous response) since asphalt binders are visco-elastic materials.

Flow Number Test. The flow number test was conducted in this study to determine the permanent deformation characteristic of the HMA mixture. The test was conducted at an effective temperature, T_{eff}, and stress level of 129.2°F and 30 psi, respectively. The test was done by applying a repeated dynamic load for several thousand repetitions on a cylindrical asphalt sample. In this study a loading cycle of 1.0 second in duration with an applied 0.1-second haversine load followed by 0.9-second rest period was used. Permanent axial strains were recorded throughout the test. The flow number was then determined as the cycle number at which tertiary flow occurs on the cumulative permanent strain curve obtained during the test (Figure 29). The flow number was used in this study as a performance criteria indicator for permanent deformation resistance of the asphalt concrete mixture.
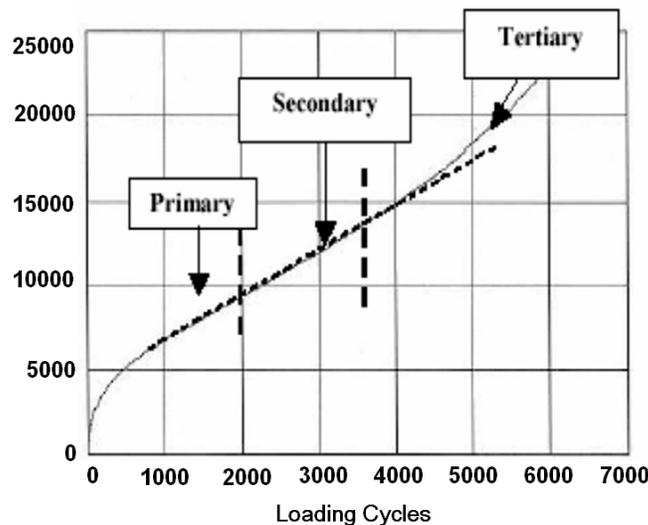
Figure 29
Relation between total cumulative plastic strain and number of load cycle

Flow Time Test. The flow time test was also conducted in this study to determine the permanent deformation characteristic of the HMA mixture. In this test, a static load is applied to the sample and the resulting strains are recorded as a function of time. The time at which the minimum rate of change of permanent deformation occurs is defined as the flow time. This test is a variation of the simple compressive creep test and is used to measure the rutting potential of asphalt mixtures.

Laboratory Test Results

        Indirect Tensile Strength Test. The ITS tests were conducted at 77°F on PMLC and PMFC samples. The ITS strength and tensile strain at failure were used in the analysis. Table 14 presents the ITS strength, the corresponding strain values, and toughness index for tested PMLC and PMFC samples. In this test, high ITS strength values at failure are desirable. The average ITS strength values were 196 and 234 psi for PMFC and PMLC samples, respectively. It is noted that PMLC samples had higher ITS strength than the PMFC samples. Those results are consistent with findings of Mohammad et al. *[35]*. In addition, the ITS strength, strain, and toughness index values obtained from this study were comparable to values obtained for Louisiana Superpave mixtures that have shown good field performance *[36]*.

Table 14
Indirect tensile strength test results

PMLC samples					PMFC samples				
Sample No.	Voids (percent)	Strength (psi)	Strain (percent)	T I	Sample No.	Voids (percent)	Strength (psi)	Strain (percent)	T I
1	7.0	200	0.39	0.77	5	7.9	166	0.97	0.91
4	6.6	269	0.62	0.79	6	5.2	226	0.77	0.86
Mean	6.8	234	0.50	0.78	Mean	6.6	196	0.87	0.89

        Indirect Tensile Resilient Modulus Test. Elastic properties of the asphalt mixes were examined by the indirect tensile resilient modulus (M_r) test. Indirect tensile resilient modulus tests were conducted on cores and PMLC samples at three different temperatures, namely 41, 77, and 104°F. The results of conducted tests are presented in Table 15. The average resilient moduli values are also shown in Figure 30. As expected, the M_r values decreased with the increase in the temperature. It is noted that in general the results are showing good resilient modulus values especially when compared to those obtained for well-performing ¾-in. Superpave mixtures reported by Mohammad et al. *[36]*.

Table 15
Indirect tensile resilient modulus test results

Temperature (°F)	PMLC samples			Core samples		
	Sample No.	Voids (percent)	Resilient Modulus (ksi)	Sample No.	Voids (percent)	Resilient Modulus (ksi)
41	5	7.3	557	1	6.8	577
	6	7.1	534	2	8.4	445
77	5	7.3	443	1	6.8	483
	6	7.1	344	2	8.4	429
104	5	7.3	267	1	6.8	362
	6	7.1	221	2	8.4	328
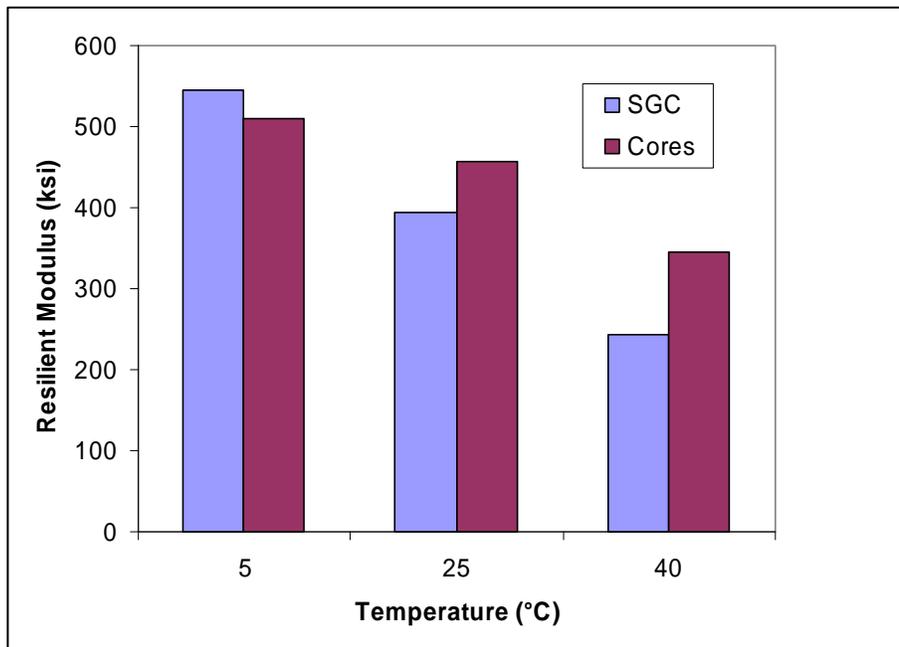
Figure 30
Resilient modulus test results

Indirect Tensile Creep Test. The indirect tensile creep test performed at 104° F provides an indication of the rutting susceptibility for the HMA mixture. Low ITC slope values are desired properties for rut resistant HMA mixtures.

66

Table 16
Indirect tensile creep test results

PMLC samples				Core samples			
Sample No.	Voids (percent)	Slope	Time to failure	Sample No.	Voids (percent)	Slope	Time to failure
2	7.4	0.26	3600[1]	3	6.1	0.43	229
3	6.9	0.33	3600[1]	4	8.5	0.50	80

[1]   Sample did not fail

Table 16 summarizes the ITC slope results for samples tested in this study. It is noted that PMLC samples have lower slope values than those of the cores. One reason that may justify this difference is the lower thicknesses of the cores. When comparing the test results with those reported by Mohammad et al. for well-performing Superpave mixtures, it is noted that the tested mixture in this study has a similar ITC slope and, hence, similar rutting susceptibility properties *[35]*.

Semi-circular Bend Test. The fracture resistance of the wearing course HMA mixture was investigated using the semi-circular bend test. The results of this test are shown in Table 17, while Figure 31 shows the linear fits of the energy needed at different notch depths. From this figure, the J_c values were calculated to be 1.32 and 1.57 kJ/m^2 for the PMLC and cored samples, respectively. It is noted that J_c data range for the wearing course HMA mixture is on the same order of magnitude as those reported by Mohammad et al. for well-performing Superpave mixtures in the state of Louisiana *[37]*.

Table 17
Semi-circular bend test

PMLC samples		Core samples	
Notch depth (in.)	Area (lb.-in.)	Notch depth (in.)	Area (lb.-in.)
1.0	13.3	1.0	14.5
1.25	9.5	1.25	10.5
1.5	4.9	1.5	5.1
E_s	-0.075	E_s	-0.084
J_c	**1.32**	**J_c**	**1.57**
R^2	0.996	R^2	0.991
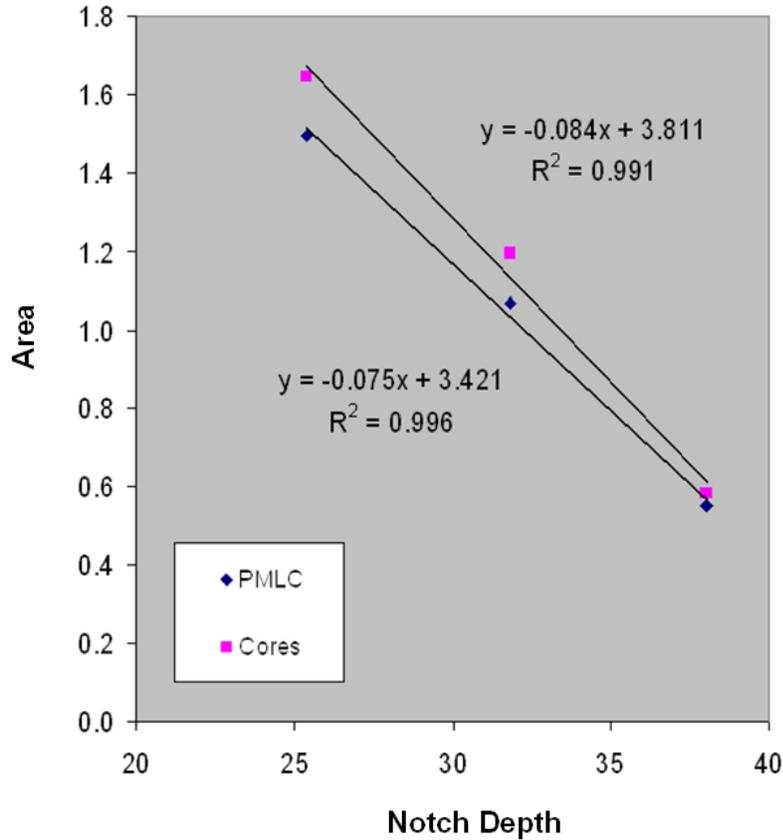
Figure 31
Semi-circular bend test results

Loaded Wheel Tracking Test. The HMA mixture was evaluated for its performance under severe load and environmental conditions using the Hamburg Type Wheel Tracking test and Asphalt Pavement Analyzer. The Hamburg Type Wheel Tracking test device measures the combined effects of rutting and moisture damage. Table 18 presents the average rut depths obtained from Hamburg Type Wheel Tracking test results for the HMA mixture under investigation. It is noted that the mixture had excellent performance with a maximum average rut depth of 0.22 in. Furthermore, no signs of stripping were detected at the end 20,000 cycles. Table 18 also shows the results obtained from the Asphalt Pavement Analyzer test. It is noted that maximum rut depth was 0.29 in., which confirms the results of the Hamburg Type Wheel Tracking test device that indicated the HMA mixture has a good permanent deformation resistance.

68

Table 18
Loaded wheel test results

Hamburg Wheel Tracking Test			Asphalt Pavement Analyzer		
Sample No.	Voids (percent)	Rut depth (in.)	Sample No.	Voids (percent)	Rut depth (mm)
1	7.4	0.22	1	7.5	0.27
3	7.5	0.2	2	6.5	0.22
			3	7.4	0.29
Mean	7.5	0.21	Mean	7.1	0.26

Flow Time and Flow Number Tests. Table 19 presents the flow number test results of individual samples along with the average flow number value. High F_N is desired for a rut-resistant mixture. It is noted an average F_N value of 1,928 was obtained for the HMA mixture considered in this study. Although this value is relatively low, it may be considered an acceptable value for low traffic mixtures. Table 20 also shows the results of the flow time test. It is noted that an average flow time value of 206 sec. was obtained for the considered HMA mixture. This value is considered to be relatively low.

Table 19
Flow number test results

Sample No.	Voids (percent)	Axial strain (micro-strain)	Flow number (cycle)
3	6.9	13596	1968
13	7.1	12577	1888
Mean	7.0	13087	1928

Table 20
Flow time test results

Sample No.	Voids (percent)	Axial strain (micro-strain)	Flow time (sec.)
2	7.4	7406	265
5	7.5	10087	146
Mean	7.5	8747	206

Frequency Sweep Test at Constant Height Test. The viscoelastic properties of asphalt mixtures were examined by performing a frequency sweep test. The material property obtained from this test was a dynamic shear modulus, also called a complex shear modulus. Dynamic shear modulus (G*) is defined as the ratio of the peak shear stress amplitude to the peak shear strain amplitude; it is a measure of total stiffness of asphalt mixtures, and it is composed of elastic and viscous components of asphalt shear modulus. The relationship between the complex shear modulus and the loading frequency, shown in Figures 32 and 33, indicates that, as the speed of loading on the specimen increases, the shear modulus increases.

The slope of the relationship between complex shear modulus and loading frequency on logarithmic scales is used to indicate the susceptibility of the mixture to both rutting and fatigue cracking. HMAs with higher slopes are more susceptible to permanent deformation. The results in Figures 32 and 33 indicate that the HMA mixture investigated in this study had the similar trend to those reported in previous studies by Mohammad et al. for good performing Superpave HMA mixtures *[36]*.
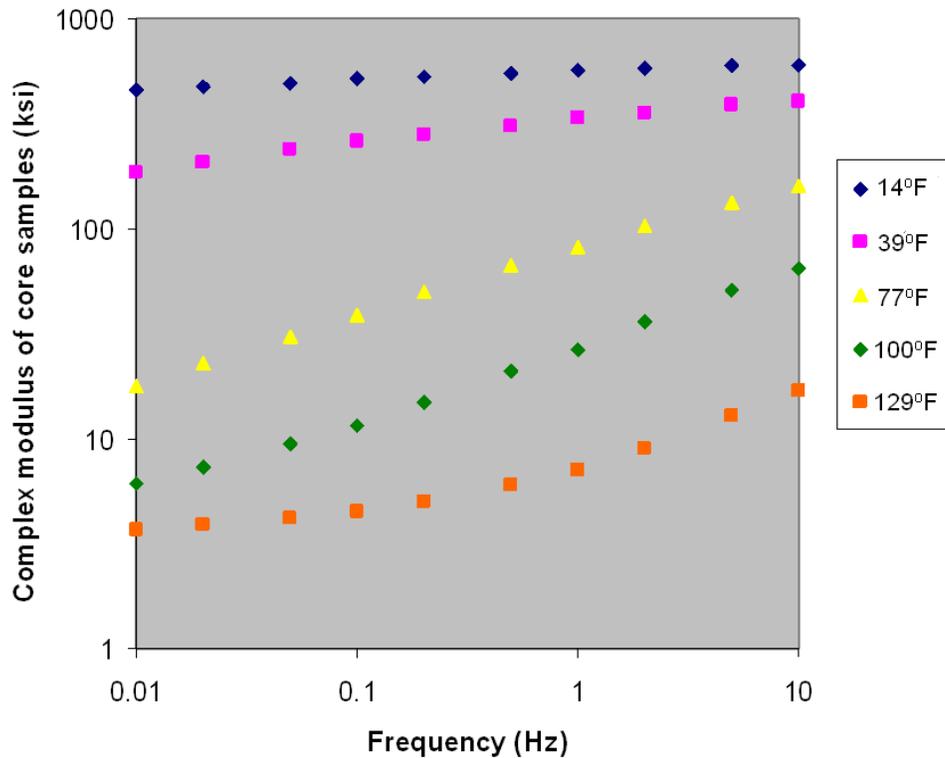
Figure 32
Frequency sweep test at constant height test results on cores
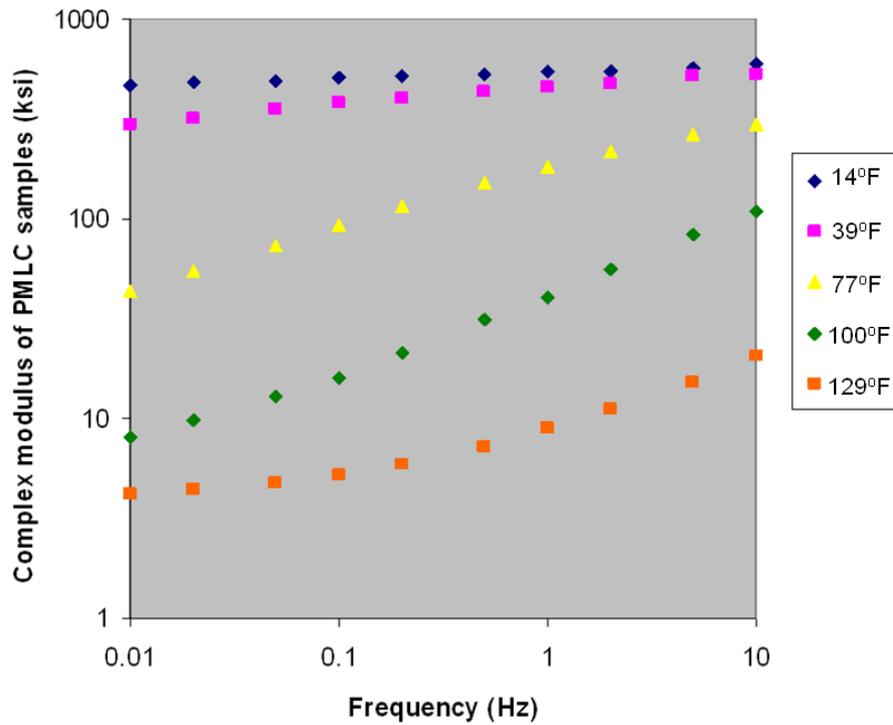
Figure 33
Frequency sweep test at constant height test results on PMLC samples

Dynamic Modulus Test. The E* and phase angle test results for the HMA mixture used in the APT experiment are presented in Table 21 and Table 22, respectively. More detail discussion has been reported in the preceding report.

Table 21
E* test moduli (ksi)

Tem.		Frequency (Hz)					
		25	10	5	1	0.5	0.1
14°F	1	3747	3651	3552	3280	3155	2856
	4	3458	3358	3263	3005	2893	2617
	8	3703	3596	3489	3219	3093	2794
	Mean	3636	3535	3435	3168	3047	2755
	STD	156	156	152	144	137	124
	COV (%)	4.3	4.4	4.4	4.6	4.5	4.5
39.2°F	1	2868	2687	2528	2139	1965	1541
	4	2615	2511	2373	2015	1883	1557
	8	2878	2630	2472	2108	1947	1564
	Mean	2787	2609	2458	2087	1931	1554
	STD	149	90	78	65	43	12
	COV (%)	5.3	3.4	3.2	3.1	2.2	0.8
77°F	1	1339	1118	959	597	482	282
	4	1283	1078	926	606	499	322
	8	1360	1137	966	631	519	316
	Mean	1328	1111	951	611	500	307
	STD	40	30	21	18	19	22
	COV (%)	3.0	2.7	2.2	2.9	3.7	7.0
100°F	1	447	301	224	118	91	54
	4	492	363	298	170	134	81
	8	496	371	292	165	128	80
	Mean	478	345	271	151	117	72
	STD	27	38	41	29	23	15
	COV (%)	5.7	11.1	15.2	19.0	19.9	21.3
129.2°F	1	112	77	61	42	36	30
	4	144	101	81	53	45	35
	8	142	99	79	54	46	37
	Mean	133	93	74	50	43	34
	STD	18	13	11	7	6	4
	COV (%)	13.5	14.3	14.9	13.3	12.8	10.6

Table 22
E* test phase angles (°)

Tem.		Frequency (Hz)					
		25	10	5	1	0.5	0.1
14°F	1	0.6	2.7	3.6	4.9	5.4	6.7
	4	0.3	2.9	3.8	5	5.5	6.7
	8	0.9	2.9	3.8	5.1	5.6	6.8
	Mean	0.6	2.8	3.7	5	5.5	6.8
	STD	0.3	0.1	0.1	0.1	0.1	0.1
	COV (%)	50.0	4.1	3.1	2.0	1.8	0.8
39.2°F	1	1.9	6.8	8.1	10.8	12.1	15.5
	4	4.3	6.7	7.9	10.1	11.2	14
	8	2.6	6.6	7.8	10.3	11.3	14.3
	Mean	2.9	6.7	7.9	10.4	11.5	14.6
	STD	1.2	0.1	0.2	0.4	0.5	0.8
	COV (%)	42.6	1.5	1.9	3.5	4.3	5.4
77°F	1	15.5	20	22.5	28.4	30.2	32
	4	14.1	17.8	20.2	25.7	27.5	30.2
	8	15.4	18.7	20.9	26.3	27.8	29.8
	Mean	15	18.8	21.2	26.8	28.5	30.6
	STD	0.8	1.1	1.2	1.4	1.5	1.2
	COV (%)	5.2	5.9	5.6	5.3	5.2	3.8
100°F	1	29.4	31.9	34	33.3	31.9	26
	4	25.5	28.1	29.1	30.1	29.6	26.1
	8	26.6	29.1	29.9	29.9	29	24.6
	Mean	27.1	29.7	31	31.1	30.2	25.5
	STD	2.0	2.0	2.6	1.9	1.5	0.8
	COV (%)	7.4	6.6	8.5	6.1	5.1	3.3
129.2°F	1	31.7	30.3	28.2	22	19.6	14.6
	4	29.1	28.6	27.1	22.8	20.7	16.1
	8	29.5	27.9	26.33	21.4	19.5	14.8
	Mean	30.1	28.9	27.2	22.1	19.9	15.2
	STD	1.4	1.2	0.9	0.7	0.7	0.8
	COV (%)	4.7	4.3	3.5	3.2	3.3	5.4